Comparison details

This document was generated by Draftable's Comparison API.

This is an independent offline version of the following comparison:

Account ID: draftable-online-compare
Comparison ID: VbQZtLPYFRDi
Left document: saveManuscript_20210224-min.pdf
Right document: template-min.pdf

Understanding the comparison

What is this?

This is a comparison of two documents. The two documents are interleaved such that the left document is displayed on odd-pages and the right document is displayed on even pages.

Is there a specific way I should view this file?

This document is intended to be viewed in Two Page Continuous mode (or sometimes called 'Two Page Scrolling'). It should open in this mode by default when using Adobe Acrobat and most popular PDF readers.

If the document opens in a different view, you can often change this in the settings. In Adobe Acrobat, go to **View > Page Display > Two Page Scrolling**.

Why are there blank pages?

Blank pages are inserted to keep both documents as aligned as much as possible.

How do I read the changes?

Text deleted from the **left** document and, hence, not in **right** document is highlighted red. Text added to the **right** document and, hence, not in **left** document is highlighted green.

Calibration and assessment of electrochemical low-cost sensors in remote alpine harsh environments

Federico Dallo[1,2], Daniele Zannoni[3], Jacopo Gabrieli[1], Paolo Cristofanelli[4], Francescopiero Calzolari[4], Fabrizio de Blasi[1], Andrea Spolaor[1], Dario Battistel[2], Rachele Lodi[1], Warren R.L. Cairns[1], Ann Mari Fjæraa[5], Paolo Bonasoni[4], and Carlo Barbante[1,2]

[1]Institute of Polar Sciences (CNR-ISP), Via Torino, 155, 30172, Venice, ITALY
[2]University Ca' Foscari of Venice, Dorsoduro 3246, 30123, Venice, ITALY
[3]Geophysical Institute, University of Bergen and Bjerknes Centre for Climate Research, Bergen, NORWAY
[4]Institute of Atmospheric Sciences and Climate (CNR-ISAC), Via P. Gobetti 101, 40129 Bologna, ITALY
[5]Norwegian Institute for Air Research (NILU), Instituttveien 18, 2007 Kjeller, NORWAY

Correspondence: Federico Dallo (federico.dallo@unive.it)

Abstract.

The present work presents the results obtained using an original open-source low-cost sensor (LCS) system developed to measure tropospheric O_3 in a remote high altitude alpine site. We conducted our study at the Col Margherita Observatory (2543 m a.s.l.), a World Meteorological Organization Global Atmosphere Watch Regional Station, located in the Italian Eastern Alps. The sensing system mounts three equivalent commercial low-cost sensors that have been calibrated using a laboratory standard (Thermo 49iPS), referenced to the Standard Reference Photometer #15 calibration scale by the WMO, before field deployment. Intra and inter-comparison between sensors and reference (Thermo 49c) have been conducted for six months from May to December 2018. The sensor's dependence on the environmental meteorological variables has been considered and discussed. The evaluation of the analytical performances of this sensing system provides an $LOD < 5$ ppb, $LOQ < 17$ ppb, LDR up to 250 ppb, intra-Pearson correlation coefficient (PCC) up to 0.96, inter-PCC > 0.8, bias > 3.5 ppb and ± 8.5 at 95% of confidence. Thanks to the first implementation of an LCS System in an alpine site, it has been demonstrated how it is possible to obtain valuable data from a low-cost instrument in a remote environment. This opens new perspectives for the adoption of a low-cost sensor network in atmospheric sciences.

Calibration and assessment of electrochemical low-cost sensors in remote alpine harsh environments

Federico Dallo[1,2], Daniele Zannoni[3], Jacopo Gabrieli[1], Paolo Cristofanelli[4], Francescopiero Calzolari[4], Fabrizio de Blasi[1], Andrea Spolaor[1], Dario Battistel[2], Rachele Lodi[1], Warren Raymond Lee Cairns[1], Ann Mari Fjæraa[5], Paolo Bonasoni[4], and Carlo Barbante[1,2]

[1]Institute of Polar Sciences (CNR-ISP), Via Torino, 155, 30172, Venice, ITALY
[2]University Ca' Foscari of Venice, Dorsoduro 3246, 30123, Venice, ITALY
[3]Geophysical Institute, University of Bergen and Bjerknes Centre for Climate Research, Bergen, NORWAY
[4]Institute of Atmospheric Sciences and Climate (CNR-ISAC), Via P. Gobetti 101, 40129 Bologna, ITALY
[5]Norwegian Institute for Air Research (NILU), Instituttveien 18, 2007 Kjeller, NORWAY

Correspondence: Federico Dallo (federico.dallo@unive.it)

Abstract.

This work presents results from an original open-source low-cost sensor (LCS) system developed to measure tropospheric O_3 in a remote high altitude alpine site. Our study was conducted at the Col Margherita Observatory (2543 m a.s.l.), in the Italian Eastern Alps. The sensor system mounts three commercial low-cost O_3/NO_2 sensors that have been calibrated

5   before field deployment against a laboratory standard (Thermo 49iPS), calibrated against the Standard Reference Photometer #15 calibration scale of the WMO. Intra and inter-comparison between the sensors and a reference instrument (Thermo 49c) have been conducted for seven months from May to December 2018. The sensors required an individual calibration, both in laboratory and in the field. The sensor's dependence on the environmental meteorological variables has been considered and discussed. We showed that it is possible to reduce the bias of one LCS by using the average coefficient values of another LCS

10   working in tandem, suggesting a way forward for the development of remote field calibration techniques. We showed that it is possible reconstruct the environmental ozone concentration during the loss of reference instrument data, in situations caused by power outages. The evaluation of the analytical performances of this sensing system provides an Limit of Detection (LOD) < 5 ppb, Limit of Quantification (LOQ) < 17 ppb, Linear Dynamic Range (LDR) up to 250 ppb, intra-Pearson correlation coefficient (PCC) up to 0.96, inter-PCC > 0.8, bias > 3.5 ppb and ± 8.5 at 95% of confidence. This first implementation of

15   a LCS system in an alpine remote location demonstrated how to obtain valuable data from a low-cost instrument in a remote environment, opening new perspectives for the adoption of low-cost sensor networks in atmospheric sciences.

1   Introduction

The troposphere is a very complex system, which is subject to continuous inputs, production and removal processes of ozone from natural phenomena and human activities (lifetime 25 days(Young et al., 2013)). In southern Europe the background tropospheric ozone concentration appears to be significantly affected by three main air mass transport processes: (i) transport of polluted air masses on regional and long-range scales; (ii) downward transport of stratospheric air masses; (iii) transport of mineral dust(Cristofanelli and Bonasoni, 2009). Large gaps remain in the surface observation network, despite many years of research and monitoring of surface ozone on regional and global scales. Especially in terms of areas without monitoring and in terms of regions that have monitoring programs but no public access to the data archive(Schultz et al., 2017). Future improvements in the database would require better data harmonization, enhanced data sharing and monitoring in data-sparse regions to develop and integrate in-situ networks, complementary to satellite instruments, in order to improve measurement accuracy and spatial/temporal sampling(O'Neill et al., 2015). Therefore covering in-situ spatial data gaps to increase the effectiveness of satellite observations, which must be calibrated using ground-base reference measurements(Organization, 2017), is necessary to achieve a better agreement between observations and models.

Tropospheric ozone was chosen for this pilot study due to its high relevance to the Earth's climate(Tørseth et al., 2012), ecosystems and human health. It is one of the most important atmospheric gases involved in photochemical reactions(Crutzen et al., 1999). Ozone is the precursor of oxidizing substances like OH^- and NO_3^- and it is a key agent determining the oxidation capacity of the troposphere(Gauss et al., 2003). Tropospheric ozone influences climate as it plays a central role in the radiative budget of the atmosphere (IPCC, 2013 p.55) and it is the third most important greenhouse gas in the free troposphere(Forster et al., 2007). Furthermore, surface ozone is a dangerous secondary pollutant causing harm to human health and ecosystems(Cooper et al., 2014; Jacobson and Jacobson, 2002).

Earth monitoring is a key aspect in improving our understanding of global processes and Climate. In this framework, remote areas, such as mountain regions, are considered reference background sites due to their sensitivity to Climate Change(Bonasoni et al., 2008; ISAC-CNR; Cristofanelli et al., 2006; Barbante et al., 2004; Gabrieli and Barbante, 2014). Therefore data coming from high-altitude observatories provide valuable insights on the Earth's Climate and are crucial for the climate communities.

At present, the problem of establishing the spatio-temporal representativeness of measurements of ozone remains a difficult task, especially in presence of great spatial variability as in the case of remote regions. Increasing the number of reference-grade observatories devoted to long-term baseline observations in the alpine area is not practicable due to the high costs of construction, maintenance and labour. Moreover, global atmospheric observatories have to be located in remote areas to reduce the influence of local source pollution, thus increasing the logistical costs and discomfort for the personnel. In this context, remote-sensing can not fully solve the spatial problem as satellite systems can only meet the established requirements if they are supported by correlative data of known quality, reliable ground-based observations and quantitative science(Dobber et al., 2006; ESA, 2020).

Emerging commercial Low-Cost Sensors (LCSs) present an unique opportunity to overcome the challenge of increasing the spatial density of monitoring sites. The rapid development and continuous improvement of low-cost technologies are

1   Introduction

The troposphere is a very complex system, which is subject to continuous inputs, production and removal processes of ozone from natural phenomena and human activities (lifetime 25 days(Young et al., 2013)). In southern Europe the background tropospheric ozone concentration appears to be significantly affected by three main air mass transport processes: (i) transport of polluted air masses on regional and long-range scales; (ii) downward transport of stratospheric air masses; (iii) transport of mineral dust(Cristofanelli and Bonasoni, 2009). Large gaps remain in the surface observation network, despite many years of research and monitoring of surface ozone on regional and global scales. Especially in terms of areas without monitoring and in terms of regions that have monitoring programs but no public access to the data archive(Schultz et al., 2017). Future improvements in the database would require better data harmonization, enhanced data sharing and monitoring in data-sparse regions to develop and integrate in-situ networks, complementary to satellite instruments, in order to improve measurement accuracy and spatial/temporal sampling(O'Neill et al., 2015). Therefore covering in-situ spatial data gaps to increase the effectiveness of satellite observations, which must be calibrated using ground-base reference measurements(Organization, 2017), is necessary to achieve a better agreement between observations and models.

Tropospheric ozone was chosen for this pilot study due to its high relevance to the Earth's climate(Tørseth et al., 2012), ecosystems and human health. It is one of the most important atmospheric gases involved in photochemical reactions(Crutzen et al., 1999). Ozone is the precursor of oxidizing substances like OH^- and NO_3^- and it is a key agent determining the oxidation capacity of the troposphere(Gauss et al., 2003). Tropospheric ozone influences climate as it plays a central role in the radiative budget of the atmosphere (IPCC, 2013 p.55) and it is the third most important greenhouse gas in the free troposphere(Forster et al., 2007). Furthermore, surface ozone is a dangerous secondary pollutant causing harm to human health and ecosystems(Cooper et al., 2014; Jacobson and Jacobson, 2002).

Earth monitoring is a key aspect in improving our understanding of global processes and Climate. In this framework, remote areas, such as mountain regions, are considered reference background sites due to their sensitivity to Climate Change(Bonasoni et al., 2008; ISAC-CNR; Cristofanelli et al., 2006; Barbante et al., 2004; Gabrieli and Barbante, 2014). Therefore data coming from high-altitude observatories provide valuable insights on the Earth's Climate and are crucial for the climate communities.

At present, the problem of establishing the spatio-temporal representativeness of measurements of ozone remains a difficult task, especially in presence of great spatial variability as in the case of remote regions. Increasing the number of reference-grade observatories devoted to long-term baseline observations in the alpine area is not practicable due to the high costs of construction, maintenance and labour. Moreover, global atmospheric observatories have to be located in remote areas to reduce the influence of local source pollution, thus increasing the logistical costs and discomfort for the personnel. In this context, remote-sensing can not fully solve the spatial problem as satellite systems can only meet the established requirements if they are supported by correlative data of known quality, reliable ground-based observations and quantitative science(Dobber et al., 2006; ESA, 2020).

Emerging commercial Low-Cost Sensors (LCSs) present an unique opportunity to overcome the challenge of increasing the spatial density of monitoring sites. The rapid development and continuous improvement of low-cost technologies are

demonstrating notable applications(Hertel et al., 2015; Hagan et al., 2018). Nowadays high-quality LCSs are beginning to play a role in areas such as modelling or emissions validation in support of state-of-the-art instrumentation and established networks(Mead et al., 2013; Win; Borrego et al., 2016, 2018; Heimann et al., 2015; Castell et al., 2015). While most Low-Cost Sensor Network applications are designed for the built environment(Mueller et al., 2017; Jiang et al., 2005; Bauman et al., 2013; Andersen and Culler, 2014; Levis et al., 2005; Andersen et al., 2017) (e.g. smart cities, indoor air quality), there is a lack of studies in remote alpine regions where data are crucial for the Climate and meteorological research community. The World Meteorological Organization Global Atmosphere Watch (WMO-GAW) recognizes that the fate of the next generation of monitoring stations could be dramatically modified by the breakthroughs of new LCSs technologies(Lewis et al., 2018), but there are still open issues to be addressed such as: (i) standardization of tools and protocols to ensure growth in the number of low-cost nodes without having to fundamentally change the LCSs network architecture, (ii) compatibility with established observing systems architecture (e.g. Zhang and Director (2010)), (iii) the simplification of the remote system management and (iv) the assurance of data quality.

In this work we aim to assess the reliability of LCSs for monitoring near-surface ozone concentrations in a remote Alpine region, focusing on the *precision*, *accuracy* and *reliability* of LCSs measurements compared with a reference instrument. We carried out two laboratory calibration experiments, in April and July 2018, in order to evaluate the LCSs performances and their stability over time in a controlled environment before field deployment. We conducted our study from March to December 2018 at the Col Margherita Atmospheric Observatory (MRG). Due to the harsh weather conditions recorded at Col Margherita, this site was considered ideal to test the performances of the LCSs in view of the modern challenge of deploying low-cost applications in real world difficult situations.

demonstrating notable applications(Hertel et al., 2015; Hagan et al., 2018). Nowadays high-quality LCSs are beginning to play a role in areas such as modelling or emissions validation in support of state-of-the-art instrumentation and established networks(Mead et al., 2013; Win; Borrego et al., 2016, 2018; Heimann et al., 2015; Castell et al., 2015). While most Low-Cost Sensor Network applications are designed for the built environment(Kim et al., 2018; Mueller et al., 2017; Jiang et al., 2005; Bauman et al., 2013; Andersen and Culler, 2014; Levis et al., 2005; Andersen et al., 2017) (e.g. smart cities, indoor air quality), there is a lack of studies in remote alpine regions where data are crucial for the Climate and meteorological research community. The World Meteorological Organization Global Atmosphere Watch (WMO-GAW) recognizes that the fate of the next generation of monitoring stations could be dramatically modified by the breakthroughs of new LCSs technologies(Lewis et al., 2018), but there are still open issues to be addressed such as: (i) standardization of tools and protocols to ensure growth in the number of low-cost nodes without having to fundamentally change the LCSs network architecture, (ii) compatibility with established observing systems architecture (e.g. Zhang and Director (2010)), (iii) the simplification of the remote system management and (iv) the assurance of data quality.

In this work we aim to assess the reliability of LCSs for monitoring near-surface ozone concentrations in a remote Alpine region, focusing on the *precision*, *accuracy* and *reliability* of LCSs measurements compared with a reference instrument. We carried out two laboratory calibration experiments, in April and July 2018, in order to evaluate the LCSs performances and their stability over time in a controlled environment before field deployment. We conducted our study from March to December 2018 at the Col Margherita Atmospheric Observatory (MRG). Due to the harsh weather conditions recorded at Col Margherita, this site was considered ideal to test the performances of the LCSs in view of the modern challenge of deploying low-cost applications in real world difficult situations.

2 Materials and Methods

2.1 Site description

Col Margherita site is characterized by an alpine climate. Considering the 2008 - 2018 time window, the annual mean temperature was 3.2 °C, with August as the warmest month with an average temperature of 11.8 °C and January as the colder month with an average temperature of -4.7 °C. The average annual rain precipitation was 1485 mm, with August as the wettest month with 161.9 mm and December as the driest month with 59.5 mm(Trentino). Although not particularly high, the location is representative of the synoptic conditions of the free troposphere as represented on maps at around 700 hPa. This is possible since the site is distant and scarcely influenced, by surrounding orographic barriers (Figure 1). The atmospheric composition of Col Margherita is linked to the air masses on a regional scale, especially during the winter, since the observatory is located above the Atmospheric Boundary Layer and therefore the local sources are not significant(Barbaro et al., 2020; Sprovieri et al., 2016). About 20 thousand people live within 10 km of the MRG observatory area and about 70 thousand within 50 km(ISTAT, 2011; Veneto, 2020; gis, b, a).

2.2 MRG Observatory description

The MRG observatory is a GAW Regional Station (WIGOS Id: 0-380-0-MRG) led by the Institute of Polar Sciences of the National Research Council of Italy (ISP-CNR). It is located on the southern-eastern side of the Italian Alps (46.36683 N, 11.79192 E), based at an altitude of 2543 meters above mean sea level (m a.s.l.), it was chosen as representative for the surrounding alpine region(Barbaro et al., 2020).

The observatory is a prefabricated insulated shelter with external dimensions of 3.00m x 2.42m x 3.22m. The observatory is equipped with a complete automatic weather station mounted on a 3 m mast (AWS: CS215-L probe, Campbell Scientific, Utah, USA; PTB110 Barometer, Vaisala, Helsinki, Finland; 05103-45 Wind Monitor, R. M. Young Company, Michigan, USA) and an UV-absorption ozone analyser (Thermo Fisher Scientific 49C, SN: 0503110399). The MRG observatory is unmanned and fully automated, it is connected to the main electrical grid and supplied with a backup solar power system with $\approx$200 Ah batteries in case of grid failure. The observatory is equipped with remote control via GSM / GPRS technology.

2.3 Ozone sensors

We used the Alphasense OX-B431 commercial passive sensor which belongs to the class of electrochemical sensors that operate in amperometric mode. The sensor generates a current that is linearly proportional to the fractional volume of the target gas. The gas sensor provides three electrodes: the working electrode (WE) where the ozone reacts and a current proportional to the ozone concentration is formed; the counter electrode (AUX) that balances the reaction of the working electrode to generate an equivalent current in the opposite direction and the reference electrode that anchors the working electrode potential to ensure that it is maintained at a fixed potential, independently from the current generated. Each sensor was purchased with its

2 Materials and Methods

2.1 Site description

Col Margherita site is characterized by an alpine climate. Considering the 2008 - 2018 time window, the annual mean temperature was 3.2 °C, with August as the warmest month with an average temperature of 11.8 °C and January as the colder month with an average temperature of -4.7 °C. The average annual rain precipitation was 1485 mm, with August as the wettest month with 161.9 mm and December as the driest month with 59.5 mm(Trentino). Although not particularly high, the location is representative of the synoptic conditions of the free troposphere as represented on maps at around 700 hPa. This is possible since the site is distant and scarcely influenced, by surrounding orographic barriers (Figure 1). Despite the location could have been affected by pollutants emitted by major cities and transported by local winds(Masiol et al., 2015; Diémoz et al., 2019), recent studies showed that the atmospheric composition of Col Margherita is related to air masses on a regional scale: in particular during winter the observatory is located above the atmospheric boundary layer so that local sources are not significant(Barbaro et al., 2020; Sprovieri et al., 2016). About 20 thousand people live within 10 km of the MRG observatory area and about 70 thousand within 50 km(ISTAT, 2011; Veneto, 2020; gis, b, a).

2.2 MRG Observatory description

The MRG observatory is a GAW Regional Station (WIGOS Id: 0-380-0-MRG) led by the Institute of Polar Sciences of the National Research Council of Italy (ISP-CNR). It is located on the southern-eastern side of the Italian Alps (46.36683 N, 11.79192 E), based at an altitude of 2543 meters above mean sea level (m a.s.l.), it was chosen as representative for the surrounding alpine region(Barbaro et al., 2020). The observatory is a prefabricated insulated shelter with external dimensions of 3.00m x 2.42m x 3.22m. The observatory is equipped with a complete automatic weather station mounted on a 3 m mast.

2.3 Low-cost sensors

We used the Alphasense OX-B431 commercial passive sensor which belongs to the class of electrochemical sensors that operate in amperometric mode. These low-cost sensors are sensitive to ozone (O_3) and nitrogen dioxide (NO_2). These oxidising sensors generate a current that is linearly proportional to the fractional volume of the target gases.

Alphasense provides a calibration certificate and reference regression coefficients for each sensor. The manufacturer declares that the calibration was conducted in a controlled environment (temperature 22 ± 3 °C, relative humidity 40 ± 15 %) using the ozone generator - Thermo Scientific Model 49i-PS (flow 0.5 $l \cdot min^{-1}$) and it was performed considering two points, zero and span (1 part per million (ppm)). The technical sheet (www.alphasense.com) reports that the sensor limit of detection is in the range of units of parts per billion (ppb), a sensitivity that is required for detecting environmental ozone concentration. The manifacturer declares that the sensor voltage output is linear up to 20 ppm of the target gas.

Three equivalent sensors were installed on the sensing system in order to evaluate intra-compatibility between measurements and calibration stability as a function of time. Laboratory calibration was performed at the CNR-ISAC headquarters (Bologna,

Figure 1. From top left to bottom. (a) Surrounding area of the Col Margherita Observatory (MRG, 46.36683 N, 11.79192 E, 2543 m a.s.l.). Geographical key points and their distance from the MRG observatory are: Passo Valles (SSE) at 2032 m a.s.l. and 3.2 km away, Cima Bocche (ESE) at 2745 m a.s.l. and 3.3 km away, Cima dell'Uomo (NNE) at 3010 m a.s.l. and 4.6 km away and Cimon della Pala (SSE) at 3184 m a.s.l. and 9.3 km away. (b) 3D aerial view of the Col Margherita (from Google Earth). (c) Satellite view of the north-east of Italy and the location of the Col Margherita Observatory (from Google Earth).
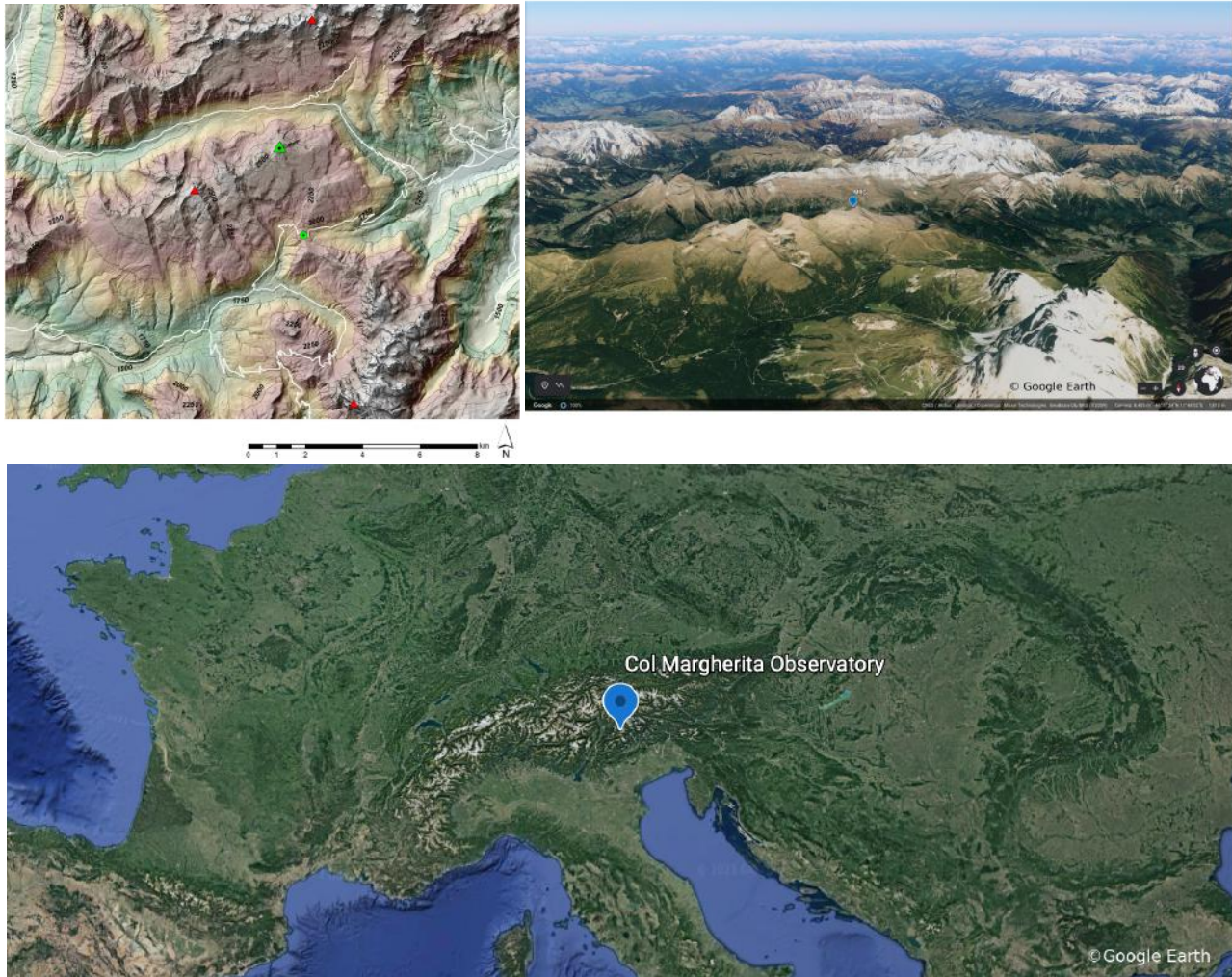
Figure 1. From top left to bottom. (a) Surrounding area of the Col Margherita Observatory (MRG, 46.36683 N, 11.79192 E, 2543 m a.s.l.). Geographical key points and their distance from the MRG observatory are: Passo Valles (SSE) at 2032 m a.s.l. and 3.2 km away, Cima Bocche (ESE) at 2745 m a.s.l. and 3.3 km away, Cima dell'Uomo (NNE) at 3010 m a.s.l. and 4.6 km away and Cimon della Pala (SSE) at 3184 m a.s.l. and 9.3 km away. (b) 3D aerial view of the Col Margherita (from Google Earth). (c) Satellite view of central Europe and the location of the Col Margherita Observatory (from Google Earth).

individual sensor board that provides a dual channel voltage output, one for the working electrode and one for the auxiliary electrode. These output pins can be interfaced with a commercial Analog to Digital Converter.

Alphasense provides a calibration certificate and reference regression coefficients for each sensor. The manufacturer declares that the calibration was conducted in a controlled environment (temperature 22 ± 3 °C, relative humidity 40 ± 15 %) using the ozone generator - Thermo Scientific Model 49i-PS (flow $0.5 \, l \cdot min^{-1}$) and it was performed considering two points, zero and span (1 part per million (ppm)). The technical sheet (www.alphasense.com) reports that the sensor limit of detection is in the range of units of parts per billion (ppb), a sensitivity that is required for detecting environmental ozone concentration. The manufacturer declares that the sensor voltage output is linear up to 20 ppm of the target gas.

Three equivalent sensors were installed on the sensing system in order to evaluate intra-compatibility between measurements and calibration stability as a function of time. Laboratory calibration was performed at the CNR-ISAC headquarters (Bologna, Italy) before field deployment. Field calibration was evaluated through inter-comparison with a reference UV-absorption O3 analyser installed at the monitoring site. The reference instrument was referred to the Standard Reference Photometer #15 (SRP-15) calibration scale(GAW Report No. 252 WCC-Empa Report No. 19/3) through an intercomparison with the calibrator hosted at the CNR-ISAC laboratory (s/n: 1404860524) in 2017, June.

2.4 Sensor node

The sensing system (Figure 2) was designed to be easily built. It consists of parts that may be purchased online and they are easy to replace in case of failure. The sensing system was composed of an IP56 enclosure with three holes for the ozone sensors and two additional holes for waterproof power and Ethernet connectors. Sensor's holes, located at the bottom side of the enclosure, were watertight with rubber O-rings seals. A bag of silica gel was placed inside the box to keep the environment dry.

The sensing system was connected to the main power grid (AC) and to the LTE router of the MRG Observatory to allow data communication and remote control. The sensing system was equipped with an uninterruptible power supply (lead acid battery and battery charge regulator) in case of AC failure. The processing unit of the sensing system was a Raspberry Pi 3b+ and the analog signal of the sensors were digitized using a ± 5V (16 bit) ADC converter (Texas Instruments ADS1115). More detailed description of the hardware components of the sensing system and the approximate cost of the system's part are reported in Supplementary Materials A.

2.5 Sensors calibration

Before field installation, LCSs were calibrated by comparing the analog voltage output of the low-cost sensors with the ozone concentration generated by an ozone calibrator (thermo scientific 49i-PS) with traceability to the WCC-Empa SRP#15 (calibration in 2017). Each sensor was installed on a specific gassing hood equipped with 1/4" barbed Swagelok fitting through which the calibration gas was fluxed using a digital mass flow meter. The calibration procedure was designed for the calibration of reference-grade instruments used in the WMO network. It consists of 21 steps in which the reference ozone (flow $0.9 \, l \cdot min^{-1}$) span from 0 to 250 ppb with a declared precision of 1 ppb and zero noise of 0.25 ppb. Each step lasts for 20

Italy) before field deployment. Field calibration was evaluated through inter-comparison with a reference UV-absorption O3 analyser installed at the monitoring site. The reference instrument was referred to the Standard Reference Photometer #15 (SRP-15) calibration scale(GAW Report No. 252 WCC-Empa Report No. 19/3) through an intercomparison with the calibrator hosted at the CNR-ISAC laboratory (s/n: 1404860524) in 2017, June. The sensing system (Figure 2) was designed to be easily built. It consists of parts that may be purchased online and they are easy to replace in case of failure. The sensing system was composed of an IP56 enclosure with three holes for the working low-cost sensors and two additional holes for waterproof power and Ethernet connectors. An additional LCS was placed inside the box as a spare sensor. It was not necessary to use it throughout the experiment. The enclosure was neither heated nor regulated nor insulated. Sensor's holes, located at the bottom side of the enclosure, were watertight with rubber O-rings seals. A bag of silica gel was placed inside the box to keep the environment dry. More detailed description of the hardware components of the sensing system and the approximate cost of the system's part are reported in Supplementary Materials S1.

2.4 Sensors calibration

Before field installation, LCSs were calibrated by comparing the analog voltage output of the low-cost sensors with the ozone concentration generated by an ozone calibrator (thermo scientific 49i-PS) with traceability to the WCC-Empa SRP#15 (calibration in 2017). Each sensor was installed on a specific gassing hood equipped with 1/4" barbed Swagelok fitting through which the calibration gas was fluxed using a digital mass flow meter. The calibration procedure was designed for the calibration of reference-grade instruments used in the WMO network. It consists of 21 steps in which the reference ozone (flow $0.9\,\mathrm{l\cdot min^{-1}}$) span from 0 to 250 ppb with a declared precision of 1 ppb and zero noise of 0.25 ppb. Each step lasts for 20 minutes and the sensor total calibration time is 7 hr. The reference concentration step sequence simulates a pseudo-random variation of ozone concentration. This procedure allows to evaluate the sensor's tolerance, ability to respond to sudden and unpredictable (small/large, increasing/decreasing) changes in the ozone concentration, to assess whether the sensor suffers from memory effect or loss of sensitivity and to estimate drifts of the instrumental response. The reproducibility and the stability of the sensors calibration parameters were evaluated performing two laboratory calibration. Three sensors (Mrg1: Alphasense Serial Number 204141855; Mrg2: S/N 204141543; Mrg3: S/N 204141544) were calibrated in Bologna between the 18th and the 19th of April 2018, deployed at Col Margherita for a month, then removed the 22nd of June and re-calibrated between the 11th and the 12th of July under the same conditions of the first calibration. The sensing system was finally re-installed at the Col Margherita Observatory on the 17th of July. During both calibration period, laboratory temperature and humidity were controlled and maintained at $\approx$22.5 °C and $\approx$50% respectively. During laboratory calibration the analog voltage output of the LCSs was recorded every second. Values were then aggregated to 1-minute averages and time-matched with the ozone concentration dataset generated (1-minute) by the reference instrument.

2.5 Field installation and data acquisition parameters

The installation of the sensing system was carried out the 25th of May 2018 at the Col Margherita Observatory. The LCSs instrument was mounted in the AWS mast, 1 m above the ground. The gas inlet through which the reference UV-absorption
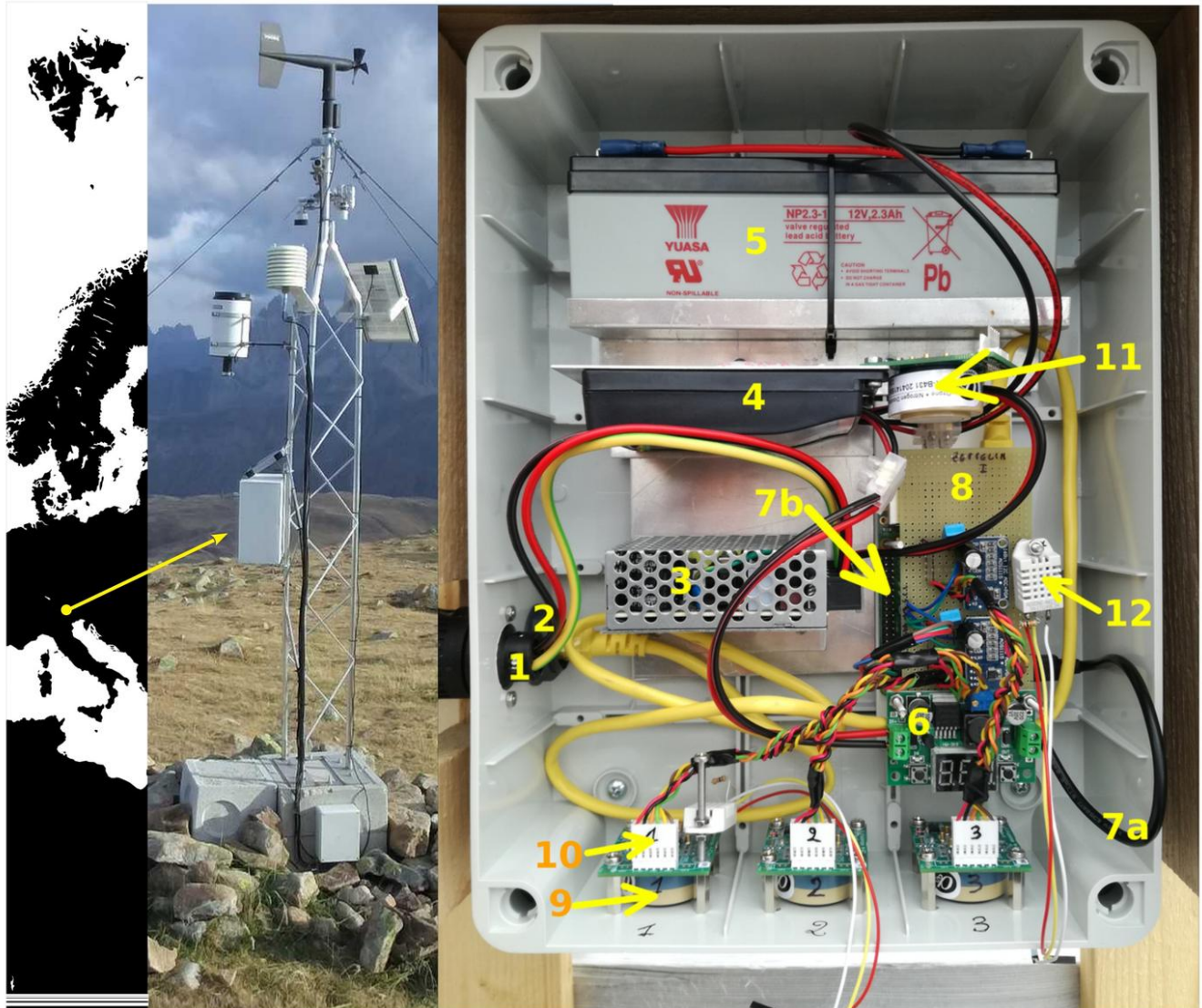
Figure 2. The low-cost sensing system and its components. 1) AC power IN, 2) Ethernet, 3) Power Supply, 4) Charge regulator, 5) Battery, 6) DC/DC converter, 7a) USB power wire, 7b) Raspberry Pi, 8) Data acquisition board, 9) Working sensor, 10) Sensor's plug, 11) Blank sensor, 12) T&RH sensor.
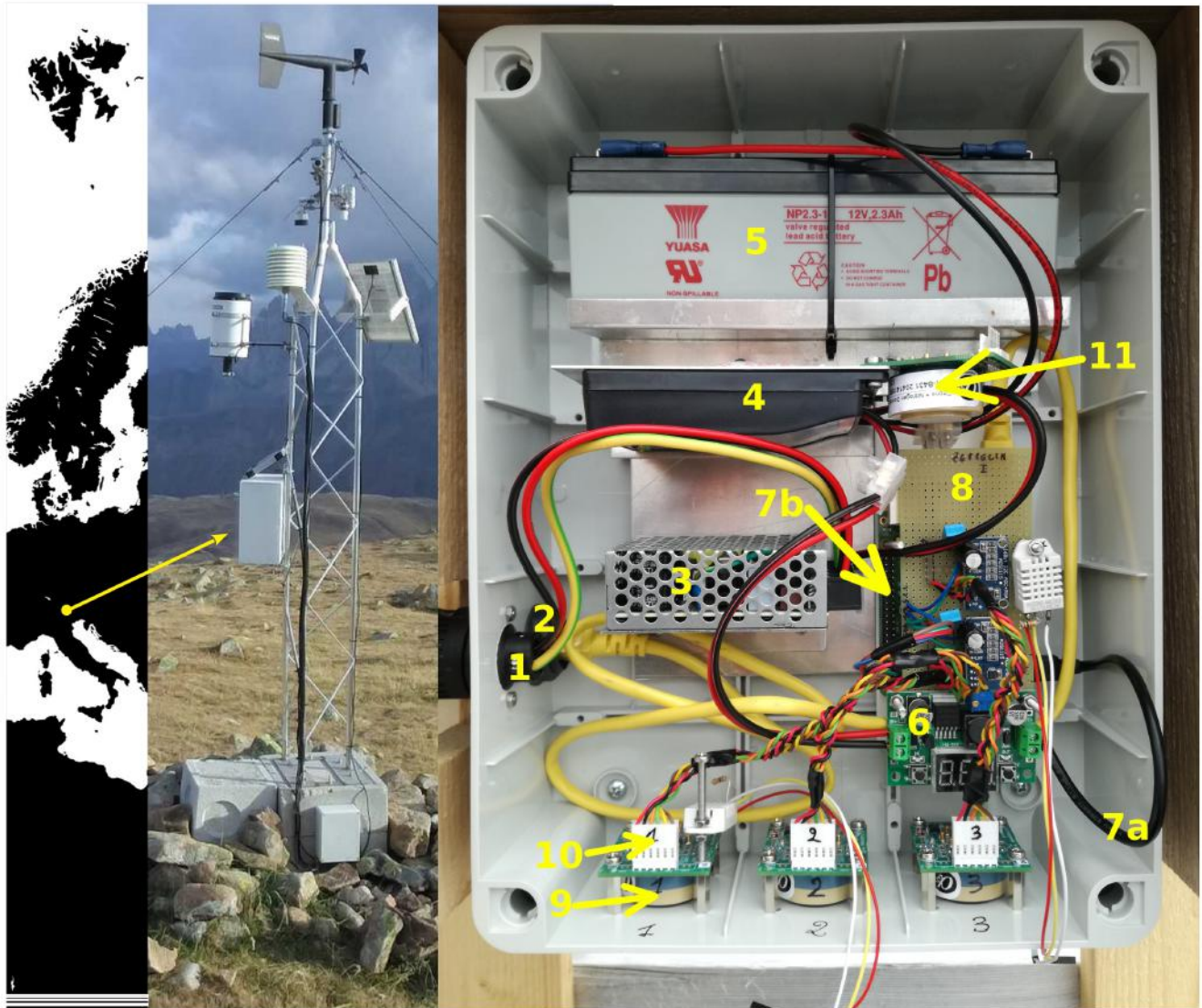
Figure 2. The low-cost sensing system and its components. 1) AC power IN, 2) Ethernet, 3) Power Supply, 4) Charge regulator, 5) Battery, 6) DC/DC converter, 7a) USB power wire, 7b) Raspberry Pi, 8) Data acquisition board, 9) Working sensor, 10) Sensor's plug, 11) Spare sensor.

minutes and the sensor total calibration time is 7 hr. The reference concentration step sequence simulates a pseudo-random variation of ozone concentration. This procedure allows to evaluate the sensor's tolerance, ability to respond to sudden and unpredictable (small/large, increasing/decreasing) changes in the ozone concentration, to assess whether the sensor suffers from memory effect or loss of sensitivity and to estimate drifts of the instrumental response. The reproducibility and the stability of the sensors calibration parameters were evaluated performing two laboratory calibration. Three sensors (Mrg1: Alphasense Serial Number 204141855; Mrg2: S/N 204141543; Mrg3: S/N 204141544) were calibrated in Bologna between the 18th and the 19th of April 2018, deployed at Col Margherita for a month, then removed the 22nd of June and re-calibrated between the 11th and the 12th of July under the same conditions of the first calibration. The sensing system was finally re-installed at the Col Margherita Observatory on the 17th of July. During both calibration period, laboratory temperature and humidity were controlled and maintained at ≈22.5 °C and ≈50% respectively. During laboratory calibration the analog voltage output of the LCSs was recorded every second. Values were then aggregated to 1-minute averages and time-matched with the ozone concentration dataset generated (1-minute) by the reference instrument.

2.6   Field installation and data acquisition parameters

The installation of the sensing system was carried out the 25th of May 2018 at the Col Margherita Observatory. The LCSs instrument was mounted in the AWS mast, 1 m above the ground. The gas inlet through which the reference UV-absorption ozone analyser sucks in the air ($\approx 0.6 \, \mathrm{l \cdot min^{-1}}$) was located on the roof of the observatory at 5 m above the ground. The comparison between the reference instrument in Col Margherita and the LCSs of ozone was performed when both the systems were running, considering the time window from May 2018 to December 2018. The analog voltage output of the LCSs was recorded every 5 seconds during the field experiment. The values were treated for the data processing as described in Sect. 2.7, then aggregated to hourly averages and finally time-matched with the reference ozone concentration dataset validated through manual and automatic data preprocessing(Naitza et al., 2020).

2.7   LCSs data processing

The LCSs raw data were preprocessed to discover possible outliers during the laboratory calibration and the field evaluation. The filter used was based on the computation of a local polynomial (R function LOESS, R Core Team; Cleveland et al. (1992)) and the median absolute deviation (MAD) between this polynomial and the measurements within a moving window. We define the outliers as measurements deviating more than 5 times the MAD from the local polynomial(Mueller et al., 2017). If the MAD was smaller than the 50% quantile of all differences (| local polynomial - measurement |) it was substituted by this value. This approach prevents the exclusion of measurements during time periods with almost no variation on the ozone concentration. We considered a time window of 20 seconds, chosen after evaluating the time series autocorrelation lag (R function ACF, R core Team; Brockwell et al. (1991)) for the laboratory calibration LCS dataset. The resulting laboratory calibration outliers were less than the 0.1% of the total LCS measurements (see Supplementary Figure B1).

A time window of 1 hr was considered before averaging the data to hourly means for the field LCS dataset. This procedure excluded less than 0.5% of 5-second raw data, mainly generated during the turning on phase of the LCS system (see

ozone analyser sucks in the air ($\approx 0.6 \ \mathrm{l \cdot min^{-1}}$) was located on the roof of the observatory at 5 m above the ground. The comparison between the reference instrument in Col Margherita and the LCSs of ozone was performed when both the systems were running, considering the time window from May 2018 to December 2018. The analog voltage output of the LCSs was recorded every 5 seconds during the field experiment. The values were treated for the data processing as described in Sect. 2.6, then aggregated to hourly averages and finally time-matched with the reference ozone concentration dataset validated through manual and automatic data preprocessing(Naitza et al., 2020).

2.6 LCSs data processing

The LCSs raw data were preprocessed to discover possible outliers during the laboratory calibration and the field evaluation. The filter used was based on the computation of a local polynomial (R function LOESS, R Core Team; Cleveland et al. (1992)) and the median absolute deviation (MAD) between this polynomial and the measurements within a moving window. We define the outliers as measurements deviating more than 5 times the MAD from the local polynomial(Mueller et al., 2017). If the MAD was smaller than the 50% quantile of all differences (| local polynomial - measurement |) it was substituted by this value. This approach prevents the exclusion of measurements during time periods with almost no variation on the ozone concentration. We considered a time window of 20 seconds, chosen after evaluating the time series autocorrelation lag (R function ACF, R core Team; Brockwell et al. (1991)) for the laboratory calibration LCS dataset. The resulting laboratory calibration outliers were less than the 0.1% of the total LCS measurements (see Supplementary Figure S2.1).

A time window of 1 hr was considered before averaging the data to hourly means for the field LCS dataset. This procedure excluded less than 0.5% of 5-second raw data, mainly generated during the turning on phase of the LCS system (see Supplementary Figure S2.2). Minutes containing less than 9 valid observations (75 %) were excluded and hourly averages were considered if there were data for at least 45 minutes (75 %). Besides, 82 hours for the Mrg2 sensor were manually excluded from the dataset. From 1AM of the 5th of November to 11PM of the 8th of November, the WE electrode of the Mrg2 sensor showed a completely different behavior compared to the other two sensors (see Supplementary Figure S2.3).

Harsh weather condition caused many periods of absence of main AC current at MRG observatory. This made the reference ozone dataset discontinuous during the summer. On September 14th, a problem on the pump of the reference instrument was diagnosed and the reference instrument was dismantled for maintenance until the 25th of October. The 29th of October we faced a power outage due to a severe storm ("Vaia", 29th of October 2018, see Supplementary Figure S5.1). Another problem with the pump of the reference instrument was encountered the 14th of December and the instrument was dismantled.

Therefore the final comparison between the reference instrument and the LCSs of ozone was performed on the $\approx$45% of the LCS's data, considering the time window from the 30th of May 2018 to the 14th of December 2018, when both the systems were running.

Evaluation of LCSs accuracy was considered skimming data if threshold value for relative humidity (RH) was overcome. We considered a multivariate ANOVA model to evaluate the effect of the meteorological variables on the LCSs measurements.

Supplementary Figure B2). Minutes containing less than 9 valid observations (75 %) were excluded and hourly averages were considered if there were data for at least 45 minutes (75 %). Besides, 82 hours for the Mrg2 sensor were manually excluded from the dataset. From 1AM of the 5th of November to 11PM of the 8th of November, the WE electrode of the Mrg2 sensor showed a completely different behavior compared to the other two sensors (see Supplementary Figure B3). Therefore the final comparison between the reference instrument and the LCSs of ozone was performed on the $\approx$45% of the LCS's data, considering the time window from May 2018 to December 2018, when both the systems were running.

Evaluation of LCSs accuracy was considered skimming data if threshold value for relative humidity (RH) was overcome. We considered a multivariate ANOVA model to evaluate the effect of the meteorological variables on the LCSs measurements.

Limit of Detection (LOD) was calculated as the average zero signal plus three times the standard deviation. Limit of Quantitation (LOQ) was calculated as the average zero signal plus ten times the standard deviation(Committee et al., 1987; for Standardization, 1994; Harris, 2010).

Limit of Detection (LOD) was calculated as the average zero signal plus three times the standard deviation. Limit of Quantitation (LOQ) was calculated as the average zero signal plus ten times the standard deviation(Committee et al., 1987; for Standardization, 1994; Harris, 2010).

3 Results

3.1 Laboratory calibration of LCSs

Laboratory calibration was performed through a linear model:

$$V_{OUT} = \beta_0 + \beta_1 \cdot [O_3] \tag{1}$$

where $V_{OUT} = V_{WE} - V_{AUX}$ is the LCS's analog output signal, $[O_3]$ is the ozone reference concentration in ppb, β_0 (mV) is the intercept, β_1 (mV $\cdot$ ppb^{-1}) is the slope. Linear model agreement between the reference and the LCS was evaluated using the Pearson correlation coefficient (PCC). Evaluation of bias was performed using the Mean Absolute Error (MAE):

$$MAE = \frac{\sum_{i=1}^{n} |e_i|}{n} \tag{2}$$

where e_i was the difference between the prediction (y_i) and the *true* value (x_i, $e_i = y_i - x_i$) and n was the number of observations.

Summary of the calibration experiments and comparison with the calibration values declared by Alphasense are reported in Table 1. As an example of the laboratory experiment, the Mrg1 calibrated ozone measurements and analog output signal registered against the reference ozone in July are shown in Figure 3 using the main and secondary y-axis respectively. We did not see a change in the analytical performances of the LCSs between the two calibration experiments (Two-sample t-test, p-value > 0.7).

The mean voltage response of Mrg1 was 18.1 ± 0.6 mV, when reference ozone concentration was 0.4 ± 0.1 ppb, and reached 100.2 ± 0.6 mV when reference ozone concentration was 249.75 ± 0.04 ppb. The precision of the Mrg1 sensor, calculated as the relative standard deviation (RSD), was $\approx 3.2\%$ close to the LOD, and decreased to $\approx 0.6\%$ for ozone concentrations higher than 200 ppb (Thompson (1988); Horwitz and Albert (1997), see Supplementary Figure D1). MAE for Mrg1 was 3.6 ppb. LOD for Mrg1 was 4 ppb. LOQ for Mrg1 was 14 ppb. The instrumental response to ozone concentration was linear in the interval considered ($R^2 = 0.998$). Through our laboratory experiment we can confirm the linear dynamic range (LDR) for Mrg1 between the LOD (4 ppb) and 250 ppb. Alphasense datasheet reports that the instrumental response of the OX-B431 sensor was linear up to 2 ppm.

The mean voltage response of Mrg2 was 0.8 ± 0.7 mV, when reference ozone concentration was 0.4 ± 0.1 ppb, and reached 89.3 ± 0.9 mV when reference ozone concentration was 250.2 ± 0.3 ppb. Precision of the Mrg2 sensor was 3.5% for values close to the LOD and decreased to 0.9% for ozone concentrations higher than 200 ppb. Mrg2's MAE was 2.5 ppb, LOD was 5 ppb, LOQ was 17 ppb and LDR was 5-250 ppb ($R^2 = 0.999$).

The mean voltage response of Mrg3 was 38.3 ± 0.9 mV, when reference ozone concentration was 0.4 ± 0.1 ppb, and reached 123.5 ± 0.9 mV when reference ozone concentration was 249.7 ± 0.2 ppb. Precision of the Mrg3 sensor was 2.6% for values close to the LOD and decreased to 0.7% for ozone concentration higher than 200 ppb. MAE for Mrg3 was 2.6 ppb. Mrg3's LOD was 3 ppb, LOQ was 9 ppb and LDR was 3-250 ppb ($R^2 = 0.998$).

3 Results

3.1 Laboratory calibration of LCSs

Laboratory calibration was performed through a linear model:

$$V_{OUT} = \beta_0 + \beta_1 \cdot [O_3] \qquad (1)$$

where $V_{OUT} = V_{WE} - V_{AUX}$ is the LCS's analog output signal, $[O_3]$ is the ozone reference concentration in ppb, β_0 (mV) is the intercept, β_1 (mV $\cdot$ ppb^{-1}) is the slope. Linear model agreement between the reference and the LCS was evaluated using the Pearson correlation coefficient (PCC). Evaluation of bias was performed using the Mean Absolute Error (MAE):

$$MAE = \frac{\sum_{i=1}^{n} |e_i|}{n} \qquad (2)$$

where e_i was the difference between the prediction (y_i) and the *true* value (x_i, $e_i = y_i - x_i$) and n was the number of observations.

Summary of the calibration experiments and comparison with the calibration values declared by Alphasense are reported in Table 1. As an example of the laboratory experiment, the Mrg1 calibrated ozone measurements and analog output signal registered against the reference ozone in July are shown in Figure 3 using the main and secondary y-axis respectively. The linear regressions of the laboratory calibrations are shown in Figure 4. We did not see a change in the analytical performances of the LCSs between the two calibration experiments (Two-sample t-test, p-value > 0.7). The mean voltage response of Mrg1 was 18.1 ± 0.6 mV, when reference ozone concentration was 0.4 ± 0.1 ppb, and reached 100.2 ± 0.6 mV when reference ozone concentration was 249.75 ± 0.04 ppb. The precision of the Mrg1 sensor, calculated as the relative standard deviation (RSD), was $\approx 3.2\%$ close to the LOD, and decreased to $\approx 0.6\%$ for ozone concentrations higher than 200 ppb (Thompson (1988); Horwitz and Albert (1997), see Supplementary Figure S4.1). MAE for Mrg1 was 3.6 ppb. LOD for Mrg1 was 4 ppb. LOQ for Mrg1 was 14 ppb. The instrumental response to ozone concentration was linear in the interval considered ($R^2 = 0.998$). Through our laboratory experiment we can confirm the linear dynamic range (LDR) for Mrg1 between the LOD (4 ppb) and 250 ppb. Alphasense datasheet reports that the instrumental response of the OX-B431 sensor was linear up to 2 ppm. Details on results for Mrg2 and Mrg3 can be found in Supplementary Materials S4.

Compared to the linear regression parameters given by the manufacturer, we obtained an average difference of about 4.2% on the intercept and an average difference of about 21.6% on the slope.

	Sensor	PCC	β_0 (mV)	β_1 (mV · ppb^{-1})	LDR (ppb)	RSD (%)	MAE (ppb)	LOD (ppb)	LOQ (ppb)	Calibration Date
Lab. Calibration	Mrg1	0.9958	18.01	0.34						2018-04-18
	Mrg1	0.9982	17.99	0.34	4-225	3.2-0.6	3.6	4	14	2018-07-11
	Mrg2	0.9971	0.05	0.38						2018-04-18
	Mrg2	0.9979	0.06	0.38	5-225	3.5-0.9	3.6	5	17	2018-07-11
	Mrg3	0.9977	36.30	0.36						2018-04-19
	Mrg3	0.9970	37.82	0.37	3-225	2.6-0.7	2.6	3	9	2018-07-12

	Sensor	MAE$_{\beta'_0,\beta_0}$	β'_0 (mV)	MAE$_{\beta'_1,\beta_1}$	β'_1 (mV · ppb^{-1})	LDR (ppb)	RSD (%)	MAE (ppb)	LOD (ppb)	LOQ (ppb)	Calibration Date
Alphasense	Mrg1	1	17	0.07	0.27	up to 2000	-	-	-	-	2018-02-06
	Mrg2	2	-2	0.10	0.28	up to 2000	-	-	-	-	2018-02-06
	Mrg3	2	36	0.07	0.30	up to 2000	-	-	-	-	2018-02-06

Table 1. In the table above are reported the linear model regression coefficients and accuracy metrics obtained during the laboratory calibration. Pearson correlation coefficient (PCC), intercept (β_0), regression coefficient (β_1), Linear Dynamic Range (LDR), Relative Standard Deviation limits (RSD), Bias (MAE), Limit of Detection (LOD) and Limit of Quantitation (LOQ). In the table below are reported the regression coefficients, intercept (β'_0) and slope (β'_1) transcribed from sensor's datasheet. Mean Absolute Error (MAE) between β'_i and β_i (averages) is given in the first two column. LCSs statistics have been performed over 300 1-sec values for each ozone concentration step, for a total of $\approx$ 6.5k calibration points per sensor. Significant digits are in accordance with the calibration datasheet.

Lab. Calibration

Sensor	PCC	β_0 (mV)	β_1 (mV·ppb^{-1})	LDR (ppb)	RSD (%)	MAE (ppb)	LOD (ppb)	LOQ (ppb)	Calibration Date
Mrg1	0.9958	18.01	0.34						2018-04-18
Mrg1	0.9982	17.99	0.34	4-225	3.2-0.6	3.6	4	14	2018-07-11
Mrg2	0.9971	0.05	0.38						2018-04-18
Mrg2	0.9979	0.06	0.38	5-225	3.5-0.9	3.6	5	17	2018-07-11
Mrg3	0.9977	36.30	0.36						2018-04-19
Mrg3	0.9970	37.82	0.37	3-225	2.6-0.7	2.6	3	9	2018-07-12

Alphasense

Sensor	MAE$_{\beta'_0,\beta_0}$	β'_0 (mV)	MAE$_{\beta'_1,\beta_1}$	β'_1 (mV·ppb^{-1})	Calibration Date
Mrg1	1	17	0.07	0.27	2018-02-06
Mrg2	2	-2	0.10	0.28	2018-02-06
Mrg3	2	36	0.07	0.30	2018-02-06

Table 1. In the table above are reported the linear model regression coefficients and accuracy metrics obtained during the laboratory calibration. Pearson correlation coefficient (PCC), intercept (β_0), regression coefficient (β_1), Linear Dynamic Range (LDR), Relative Standard Deviation limits (RSD), Bias (MAE), Limit of Detection (LOD) and Limit of Quantification (LOQ). In the table below are reported the regression coefficients, intercept (β'_0) and slope (β'_1) transcribed from sensor's datasheet. Mean Absolute Error (MAE) between β'_i and β_i (averages) is given in the first two column. LCSs statistics have been performed over 300 1-sec values for each ozone concentration step, for a total of $\approx$ 6.5k calibration points per sensor. Significant digits are in accordance with the calibration datasheet.

Figure 3. After calibration, voltage data (V_{OUT}) of the low-cost sensor is expressed in ppb (black) and compared to the reference ozone concentration (green). Sensor's ozone concentration obtained using the intercept and the regression coefficient provided by Alphasense are also shown (gray). Calibration date: 2018-07-11.

3.2 Field experiment

Field measurements were conducted from the 30th of May 2018 to the 14th of December 2018. We measured about 4800 hourly data that were collected in a wide range of environmental temperature ($^\circ$C), pressure (hPa), wind speed ($\text{m} \cdot \text{s}^{-1}$) and RH (%) as summarized in Table 2.

	Temperature ($^\circ C$)	Relative Humidity (%)	Atmospheric Pressure (hPa)	Wind Speed (m/s)
min	-16.7	10	728.8	0.0
median	5.5	84.1	753.2	3.1
mean	4.0	79.1	753.6	3.8
max	18.3	100	771.7	34.9

Table 2. Meteorological data at Col Margherita evaluated from the 30th of May 2018 to the 14th of December 2018.

3.3 Correlation and bias between LCSs. Intra-comparison

A first estimate to verify that the LCSs were in agreement with each other during field measuring was done calculating their (PCC) and bias, referred as MAE, throughout the period considered, and their variation trends over time. A summary of the
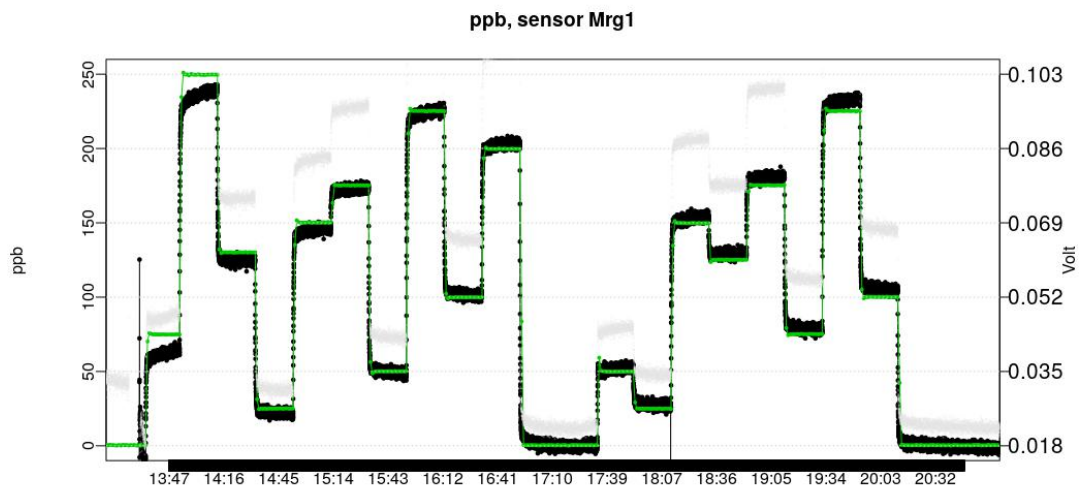
Figure 3. After calibration, voltage data (V_{OUT}) of the low-cost sensor is expressed in ppb (black) and compared to the reference ozone concentration (green). Sensor's ozone concentration obtained using the intercept and the regression coefficient provided by Alphasense are also shown (gray). Calibration date: 2018-07-11.
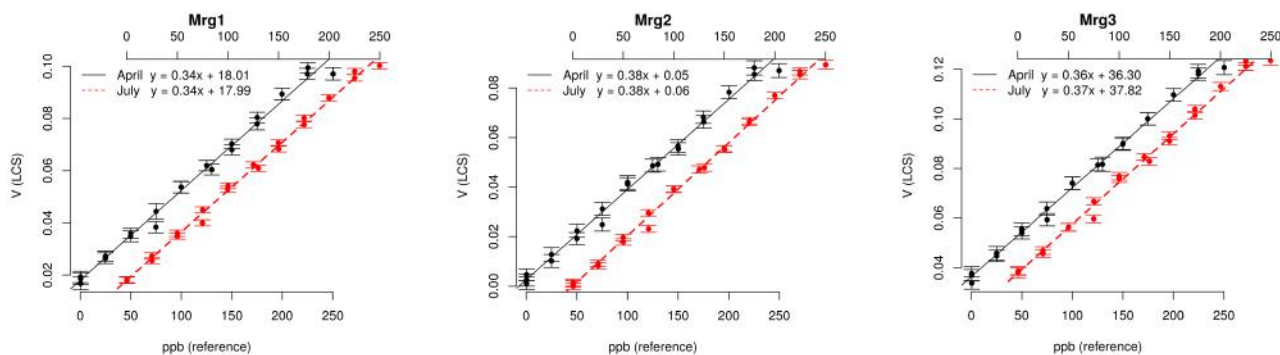
Figure 4. Laboratory calibration of the low-cost sensors. Linear regressions obtained during April (black) and July (red) are shown. From left to right are reported the results for sensors Mrg1, Mrg2 and Mrg3 respectively. To improve the visibility of the pictures two shifted x axis are given: the bottom axis refers to the April experiment while the upper axis refers to the July experiment.

3.2 Field experiment

Field measurements were conducted from the 30th of May 2018 to the 14th of December 2018. We measured about 4800 hourly data that were collected in a wide range of environmental temperature ($^\circ$C), pressure (hPa), wind speed ($\mathrm{m \cdot s^{-1}}$) and RH (%) as summarized in Table 2.

	Temperature ($^\circ C$)	Relative Humidity (%)	Atmospheric Pressure (hPa)	Wind Speed (m/s)
min	-16.7	10	728.8	0.0
median	5.5	84.1	753.2	3.1
mean	4.0	79.1	753.6	3.8
max	18.3	100	771.7	34.9

Table 2. Summary of the meteorological data (Temperature, Relative Humidity, Atmospheric Pressure and Wind Speed) recorded at Col Margherita during the field experiment, from the 30th of May 2018 to the 14th of December 2018.

3.3 Correlation and bias between LCSs. Intra-comparison

A first estimate to verify that the LCSs were in agreement with each other during field measuring was done calculating their (PCC) and bias, referred as MAE, throughout the period considered, and their variation trends over time. A summary of the inter-PCC and inter-MAE trends are reported in (Table 3). The comparison is consistent except for the month of October. Out of the 744 hourly observations collected during the month, only 59 were considered for the analysis. From the 25th to the 28th of October, when both the LCS system and the reference instrument were working (see subsection 2.6). Since there were no signs of malfunctions and given the low environmental variability of the ozone concentration during the three days analysed (29 ppb < O_3 < 47 ppb calculated by the reference instrument and 25 ppb < O_3 < 46 ppb calculated averaging the LCSs measurements), we hypothesized that the low correlation value between LCSs could have been due to the inherent variability of the sensors' measurements. Indeed, if all the 744 LCSs hourly observations of October were considered, we could have calculated: $PCC_{1,2} = 0.86, PCC_{1,3} = 0.85, PCC_{2,3} = 0.86$, a result consistent with the other periods described in Table 3.

The statistical analysis over 1772 hourly observations from the 30th of May to the 14th of December gives $PCC_{1,2} = 0.90$, $PCC_{1,3} = 0.95$ and $PCC_{2,3} = 0.93$ while $MAE_{1,2} = 4.4$ ppb, $MAE_{1,3} = 2.8$ ppb and $MAE_{2,3} = 4.4$ ppb.

3.4 Correlation and bias between low-cost sensors and reference. Inter-comparison

We measured the correlation and the bias between the LCSs and the reference instrument to evaluate the performances of the LCSs in a real case scenario where there could be no possibility to improve the laboratory calibration model. In addition to the calculation of the MAE we consider also the Root Mean Square Error (RMSE) and, to highlight the sign of the bias, the Mean

inter-PCC and inter-MAE trends are reported in (Table 3). The statistical analysis over the total 1772 hourly observations from the 30th of May to the 14th of December gives $PCC_{1,2} = 0.90$, $PCC_{1,3} = 0.95$ and $PCC_{2,3} = 0.93$ while $MAE_{1,2} = 4.4$ ppb, $MAE_{1,3} = 2.8$ ppb and $MAE_{2,3} = 4.4$ ppb.

	Total	Jun	Jul	Aug	Sep	Oct	Nov	Dec
$PCC_{1,2}$	0.90	0.68	0.85	0.92	0.87	0.79	0.87*	0.87
$PCC_{1,3}$	0.95	0.87	0.95	0.96	0.92	0.62	0.85	0.84
$PCC_{2,3}$	0.93	0.86	0.84	0.91	0.86	0.57	0.79*	0.75
$MAE_{1,2}$	4.39	6.69	5.72	3.35	3.30	4.14	3.48*	4.50
$MAE_{1,3}$	2.84	4.41	2.78	1.96	2.01	2.49	2.45	2.85
$MAE_{2,3}$	4.44	3.60	5.12	3.50	3.24	4.89	4.87*	7.00
Obs. nr.	1772	387	77	248	208	59	521	236

Table 3. Stability of LCSs intra-correlation (PCC) and bias (MAE) considering the period from the 30th of May to the 14th of December 2018. *Due to the malfunction of the Mrg2 sensor, 82 hourly observations from 2020-11-05 to 2020-11-08 of this sensor have been excluded from the LCSs dataset.

3.4 Correlation and bias between low-cost sensors and reference. Inter-comparison

We measured the correlation and the bias between the LCSs and the reference instrument to evaluate the performances of the LCSs in a real case scenario where there could be no possibility to improve the laboratory calibration model. In addition to the calculation of the MAE we consider also the Root Mean Square Error (RMSE) and, to highlight the sign of the bias, the Mean Bias Error (MBE), defined as follows:

$$RMSE = \sqrt{\frac{\sum_{i=1}^{n}(e_i)^2}{n}} \tag{3}$$

$$MBE = \frac{\sum_{i=1}^{n} e_i}{n} \tag{4}$$

In this contest the *true* value is the ozone measured by the reference instrument in Col Margherita. The statistical analysis, considering both the whole dataset and the trend of each sensor, is reported in Table 4. On average, the PCC between the sensors and the reference was ≈ 0.8, with the smallest values registered in December. The average MAE was ≈ 5 ppb and RMSE was ≈ 7 ppb. The bias was not constant through the period. It was larger during summer and it decreased during autumn, with the MBE showing a change in the sign. Probable causes that might affect the accuracy of the LCS measurements could be the environmental temperature and relative humidity, whose dependence is also described in the sensor datasheet.

	Total	Jun	Jul	Aug	Sep	Oct	Nov	Dec
$PCC_{1,2}$	0.90	0.68	0.85	0.92	0.87	0.79	0.87*	0.87
$PCC_{1,3}$	0.95	0.87	0.95	0.96	0.92	0.62	0.85	0.84
$PCC_{2,3}$	0.93	0.86	0.84	0.91	0.86	0.57	0.79*	0.75
$MAE_{1,2}$	4.39	6.69	5.72	3.35	3.30	4.14	3.48*	4.50
$MAE_{1,3}$	2.84	4.41	2.78	1.96	2.01	2.49	2.45	2.85
$MAE_{2,3}$	4.44	3.60	5.12	3.50	3.24	4.89	4.87*	7.00
Obs. nr.	1772	387	77	248	208	59	521	236

Table 3. Stability of LCSs intra-correlation ($PCC_{i,j}$) and bias ($MAE_{i,j}$) considering the period from the 30th of May to the 14th of December 2018. The indices "i" and "j" are referred to the LCSs between which the comparison is made, e.g. $PCC_{1,2}$ is the Pearson Correlation between the sensors Mrg1 and Mrg2. For each statistical metrics are reported its total, monthly values, and the number of hourly observations that are used to perform the calculation. *Due to the malfunction of the Mrg2 sensor, 82 hourly observations from 2020-11-05 to 2020-11-08 of this sensor have been excluded from the LCSs dataset.

215 Bias Error (MBE), defined as follows:

$$RMSE = \sqrt{\frac{\sum_{i=1}^{n}(e_i)^2}{n}}$$ (3)

$$MBE = \frac{\sum_{i=1}^{n} e_i}{n}$$ (4)

In this contest the *true* value is the ozone measured by the reference instrument in Col Margherita. The statistical analysis,
220 considering both the whole dataset and the trend of each sensor, is reported in Table 4. On average, the PCC between the sensors and the reference was ≈ 0.8, with the smallest values registered in December. The average MAE was ≈ 5 ppb and RMSE was ≈ 7 ppb. The bias was not constant through the period. It was larger during summer and it decreased during autumn, with the MBE showing a change in the sign. Probable causes that might affect the accuracy of the LCS measurements could be the environmental temperature and relative humidity, whose dependence is also described in the sensor datasheet and further
225 investigated in Section 3.4.1 and Section 3.5.

We observed cases with poor agreement. Perhaps lower ozone concentrations and/or low environmental variation of ozone concentrations encountered in the mid winter periods influenced the data quality from the sensors or even the reference instrument. This could explain the low correlation observed during December. Also, as discussed in subsection 3.3, we hypothesized that the low correlation value between LCSs and reference during October could have been due to the short amount of period
230 where both systems were running. The case of June for Mrg2 and for all the LCSs during July were peculiar. Perhaps a role played by the temperature difference between the inside and outside of the box could explain the lower correlation.

		Total	Jun	Jul	Aug	Sep	Oct	Nov∗	Dec
Mrg1	PCC	0.86	0.78	0.47	0.73	0.62	0.61	0.67	0.37
	MAE	4.83	5.92	9.01	6.30	4.47	2.73	3.45	3.69
	RMSE	6.32	7.21	11.27	8.08	5.76	3.63	4.35	4.74
	MBE	1.83	4.86	7.62	4.27	1.56	0.15	-0.59	-2.24
Mrg2	PCC	0.79	0.36	0.46	0.75	0.70	0.65	0.64	0.36
	MAE	6.44	11.36	5.18	4.64	3.27	4.39	5.03	6.84
	RMSE	8.76	14.33	6.74	6.26	4.33	5.21	6.11	7.99
	MBE	0.76	10.75	2.70	2.01	-0.63	-3.92	-3.58	-6.71
Mrg3	PCC	0.84	0.63	0.49	0.76	0.68	0.32	0.70	0.43
	MAE	5.27	9.00	8.07	6.27	4.19	3.77	3.06	3.00
	RMSE	7.13	10.74	10.42	7.89	5.32	4.76	3.97	3.68
	MBE	3.12	8.35	5.47	4.31	1.10	0.50	0.39	0.27
	1h-obs. nr.	1772	387	77	248	208	59	521	236

Table 4. Inter-correlation and bias between the LCSs calibrated in the laboratory and the reference. The sum of the hourly observations in the monthly analysis differ with the total 1793 observations by the data from 31th May.

3.4.1 Relative humidity threshold

230 The sensor's datasheet reports that the sensors must operate in the RH range from 15% to 90%. Established that excluding data collected outside the interval does not improve the correlation and accuracy metrics between the LCSs and the reference and considering the poor improvement obtained, we did not perform any RH correction on LCSs measurements at the MRG observatory.

3.5 Environmental low-cost sensors model

235 We evaluated the relationship between the bias and the temperature, relative humidity, atmospheric pressure, solar radiation, wind speed and wind direction to further investigate which meteorological variables were contributing to the bias (e_i) between the LCSs (O_3^{lcs}) and the reference ozone concentration (O_3^R). Figure 4 shows the correlation plots for temperature, relative humidity and LCSs signal while the remaining plots for the non correlating variables are reported in the Supplementary Figure E2. The bias showed a correlation trend with the air temperature (PCC ≈ 0.53, p-value $< 2e - 16$) and relative humidity 240 (PCC ≈ 0.45, p-value $< 2e - 16$), while no evidence of correlation was shown with the incident solar radiation (PCC ≈ 0.05, p-value ≈ 0.1), the atmospheric pressure (PCC ≈ 0.24, p-value ≈ 0.3), the wind speed (PCC ≈ -0.22, p-value ≈ 0.1) or the

		Total	Jun	Jul	Aug	Sep	Oct	Nov∗	Dec
Mrg1	PCC	0.86	0.78	0.47	0.73	0.62	0.61	0.67	0.37
	MAE	4.83	5.92	9.01	6.30	4.47	2.73	3.45	3.69
	RMSE	6.32	7.21	11.27	8.08	5.76	3.63	4.35	4.74
	MBE	1.83	4.86	7.62	4.27	1.56	0.15	-0.59	-2.24
Mrg2	PCC	0.79	0.36	0.46	0.75	0.70	0.65	0.64	0.36
	MAE	6.44	11.36	5.18	4.64	3.27	4.39	5.03	6.84
	RMSE	8.76	14.33	6.74	6.26	4.33	5.21	6.11	7.99
	MBE	0.76	10.75	2.70	2.01	-0.63	-3.92	-3.58	-6.71
Mrg3	PCC	0.84	0.63	0.49	0.76	0.68	0.32	0.70	0.43
	MAE	5.27	9.00	8.07	6.27	4.19	3.77	3.06	3.00
	RMSE	7.13	10.74	10.42	7.89	5.32	4.76	3.97	3.68
	MBE	3.12	8.35	5.47	4.31	1.10	0.50	0.39	0.27
	1h-obs. nr.	1772	387	77	248	208	59	521	236

Table 4. Inter-correlation and bias between the LCSs, calibrated in the laboratory, and the reference. Statistical metrics considered are the Pearson correlation coefficient (PCC), Mean Absolute Error (MAE), Root Mean Square Error ($RMSE$) and Mean Bias Error (MBE). For each statistical metrics are reported its total, monthly values, and the number of hourly observations that are used to perform the calculation. The sum of the hourly observations in the monthly analysis differ with the total 1793 observations by the data from the 31th of May to the 14th of June. *Due to the malfunction of the Mrg2 sensor, 82 hourly observations from 2020-11-05 to 2020-11-08 of this sensor have been excluded from the LCSs dataset.

3.4.1 Relative humidity threshold

The Alphasense Application Note 106 (AAN 106) reports that the low-cost sensors must operate in the RH range from 15% to 90%. We evaluated that the exclusion of the observations collected outside the RH interval does not improve the correlation and
235 accuracy metrics between the LCSs and the reference instrument. Thus, considering the poor improvement obtained through skimming, we did not exclude further LCSs measurements from the dataset.

3.5 Environmental low-cost sensors model

We evaluated the relationship between the bias and the temperature, relative humidity, atmospheric pressure, solar radiation, wind speed and wind direction to further investigate which meteorological variables were contributing to the bias (e_i) between
240 the LCSs (O_3^{lcs}) and the reference ozone concentration (O_3^R). Figure 5 shows the correlation plots for temperature, relative humidity and LCSs signal while the remaining plots for the non correlating variables are reported in the Supplementary Figure S5.6. The bias showed a correlation trend with the air temperature (PCC ≈ 0.53, p-value $< 2e-16$) and relative humidity

wind direction (PCC ≈ -0.10, p-value ≈ 0.4). We finally observed that the bias was dependent on the sensor signal itself (PCC ≈ 0.55, $p < 2e - 16$).
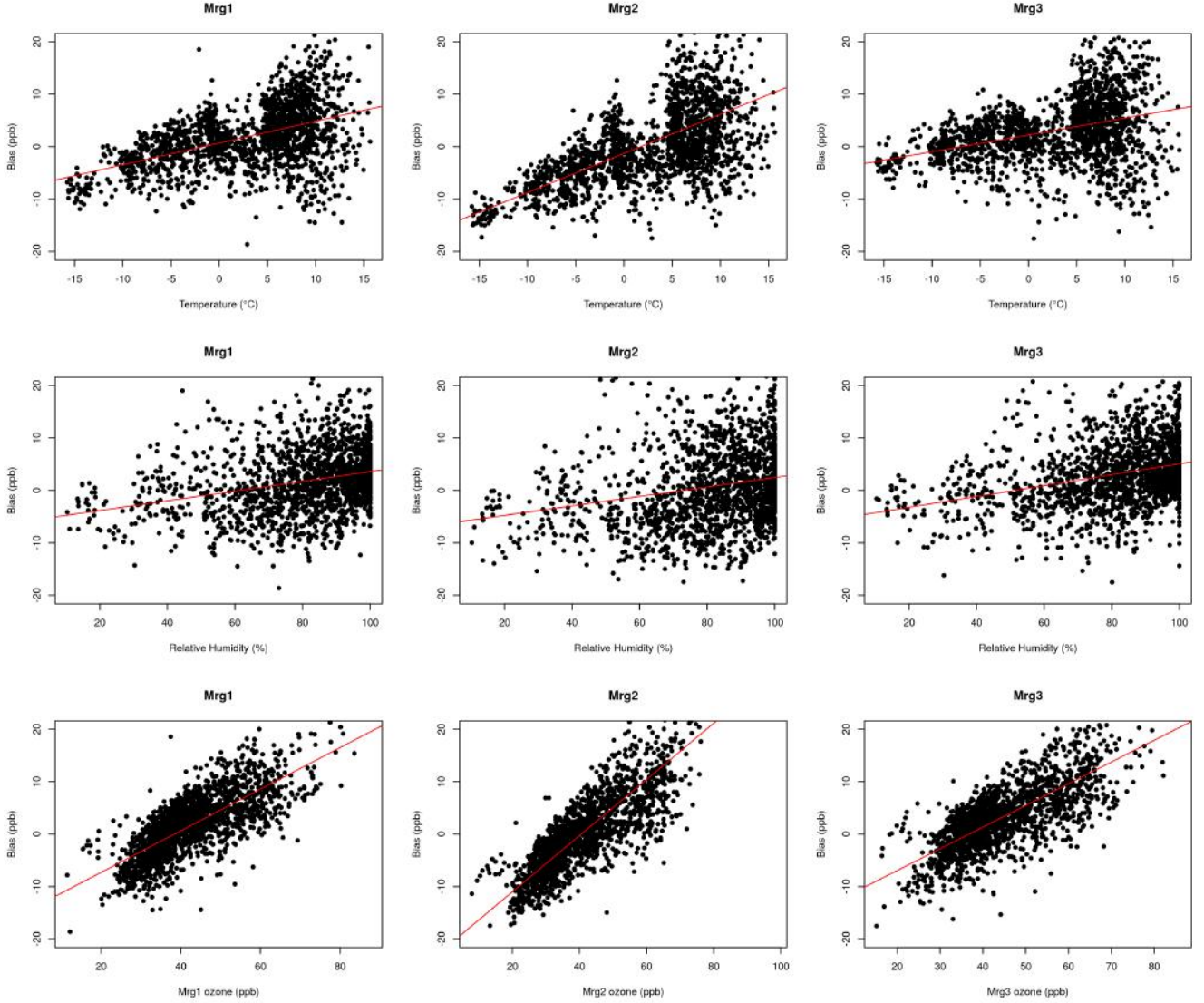
Figure 4. The environmental variables with a non negligible linear correlation with the LCS bias.

We considered the following statistical multivariate linear model to evaluate the sensors bias under specific meteorological conditions and LCS signal, implementing in the model only the explanatory variables as previously described:

$$e_j = a_{0,j} + a_{1,j}T + a_{2,j}RH + a_{3,j}O_3^{lcs,j} \tag{5}$$

(PCC ≈ 0.45, p-value < $2e − 16$), while no evidence of correlation was shown with the incident solar radiation (PCC ≈ 0.05, p-value ≈ 0.1), the atmospheric pressure (PCC ≈ 0.24, p-value ≈ 0.3), the wind speed (PCC ≈ −0.22, p-value ≈ 0.1) or the wind direction (PCC ≈ −0.10, p-value ≈ 0.4). We finally observed that the bias was dependent on the sensor signal itself (PCC ≈ 0.55, $p < 2e − 16$).
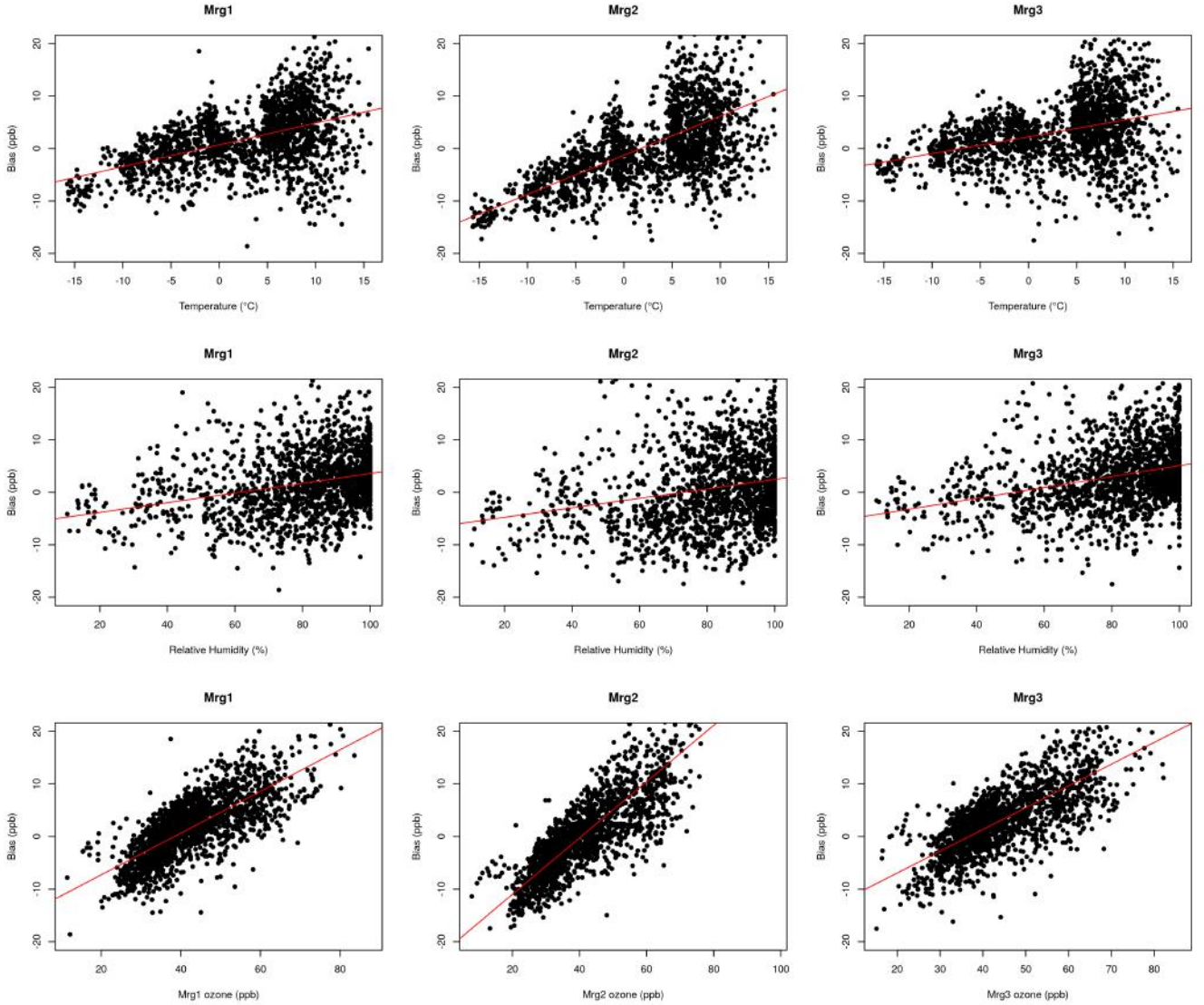
Figure 5. The environmental variables with a non negligible linear correlation with the LCS bias.

where bias (e_j, j=1,2,3) is the difference in the ozone concentration measurement between the j-esimo LCS and the reference, $a_{i,j}$ denote the model coefficients, T is the ambient air temperature, RH is the relative humidity and $O_3^{lcs,j}$ are the j-esimo LCS ozone reading obtained from Equation 1.

250   We thus used Equation 5 to improve the laboratory calibration model and to achieve a better estimation of the field (F) ozone concentration measured by the j-esimo low-cost sensors ($O_3^{F,j}$):

$$O_3^{F,j} = O_3^{lcs,j} - e_j \tag{6}$$

3.6   Performance of the model

We considered three case scenarios to evaluate the performance of the model. A summary of the values obtained are reported
255   in Table 5.

3.6.1   Scenario 1

The first scenario considered the whole reference dataset to model the bias and correct the LCSs measurements. The inter-correlation between the LCSs and the reference improved by $\approx 1\%$. The accuracy between the LCSs measurements and the reference improved by $\approx 60\%$ lowering the average bias (MAE) from ≈ 5.5 to ≈ 3.2 ppb, with the 50% of the bias distribution
260   between $\approx \pm 2.5$ ppb and the 95% between $\approx \pm 8.5$ ppb (Figure 5). The corrected LCSs dataset, obtained by the continuous calibration of the LCSs in Col Margherita, could be used to reconstruct the environmental ozone concentration in case of loss of reference data, a situation that may occur due to power outages or during the instrumental calibration when the reference instrument is not present at the observatory. During our experiment we obtained 1556 1-hr additional ozone measurements, considering the time periods where the LCSs and the AWS were collecting data (Figure 6).

265   #### 3.6.2   Scenario 2

A second scenario still considered the whole reference dataset, but it aims to evaluate the intra-compatibility of the LCSs bias model. This might be useful if considering the use of the bias model of one low-cost sensor for the calibration of another low-cost sensor. This approach opens the possibility of performing a remote calibration in the surrounding area of the Col Margherita. A remote calibration allows the deployment of a local sensor network where remote standalone sensor's signal
270   is corrected using the bias model studied in a location where a reference instrument is always present. We compared the coefficients of the bias model of each low-cost sensor. Subsequently, we evaluated the accuracy between one of the LCSs and the reference, correcting its dataset using the averaged model coefficients of all the three LCSs (scenario 2a). Next, we evaluated the accuracy between a LCS and the reference, correcting its LCS dataset using the averaged value of the other two LCSs coefficients (scenario 2b). The average value of the intercept coefficient (a_0) is -27.76 $\pm$ 8.94%. The average value of
275   the temperature coefficient (a_1) is 0.26 $\pm$ 8.11%. The average value of the RH coefficient (a_2) is 0.11 $\pm$ 5.41% and the average values of the LCS coefficient (a_3) is 0.45 $\pm$ 11.32%.

We considered the following statistical multivariate linear model to evaluate the sensors bias under specific meteorological conditions and LCS signal, implementing in the model only the explanatory variables as previously described:

$$e_j = a_{0,j} + a_{1,j}T + a_{2,j}RH + a_{3,j}O_3^{lcs,j} \tag{5}$$

250   where bias (e_j, j=1,2,3) is the difference in the ozone concentration measurement between the j-th LCS and the reference, $a_{i,j}$ denote the model coefficients, T is the ambient air temperature, RH is the relative humidity and $O_3^{lcs,j}$ are the j-th LCS ozone reading obtained from Equation 1.

We thus used Equation 5 to improve the laboratory calibration model and to achieve a better estimation of the field (F) ozone concentration measured by the j-th low-cost sensors ($O_3^{F,j}$):

255    $$O_3^{F,j} = O_3^{lcs,j} - e_j \tag{6}$$

3.6   Performance of the model

We considered three case scenarios to evaluate the performance of the model. A summary of the values obtained are reported in Table 5.

3.6.1   Scenario 1

260   The first scenario considered the whole reference dataset to model the bias and correct the LCSs measurements. The inter-correlation between the LCSs and the reference improved by $\approx 1\%$. The accuracy between the LCSs measurements and the reference improved by $\approx 60\%$ lowering the average bias (MAE) from ≈ 5.5 to ≈ 3.2 ppb, with the 50% of the bias distribution between $\approx \pm 2.5$ ppb and the 95% between $\approx \pm 8.5$ ppb (Figure 6). The corrected LCSs dataset, obtained by the continuous calibration of the LCSs in Col Margherita, could be used to reconstruct the environmental ozone concentration in case of loss

265   of reference data, a situation that may occur due to power outages or during the instrumental calibration when the reference instrument is not present at the observatory. During our experiment we obtained 1556 1-hr additional ozone measurements, considering the time periods where the LCSs and the AWS were collecting data (Supplementary Materials S5).

3.6.2   Scenario 2

A second scenario still considered the whole reference dataset, but it aims to evaluate the intra-compatibility of the LCSs bias

270   model. This might be useful if considering the use of the bias model of one low-cost sensor for the calibration of another low-cost sensor. This approach opens the possibility of performing a remote calibration in the surrounding area of the Col Margherita. A remote calibration allows the deployment of a local sensor network where remote standalone sensor's signal is corrected using the bias model studied in a location where a reference instrument is always present. We compared the coefficients of the bias model of each low-cost sensor. Subsequently, we evaluated the accuracy between one of the LCSs

275   and the reference, correcting its dataset using the averaged model coefficients of all the three LCSs (scenario 2a). Next, we
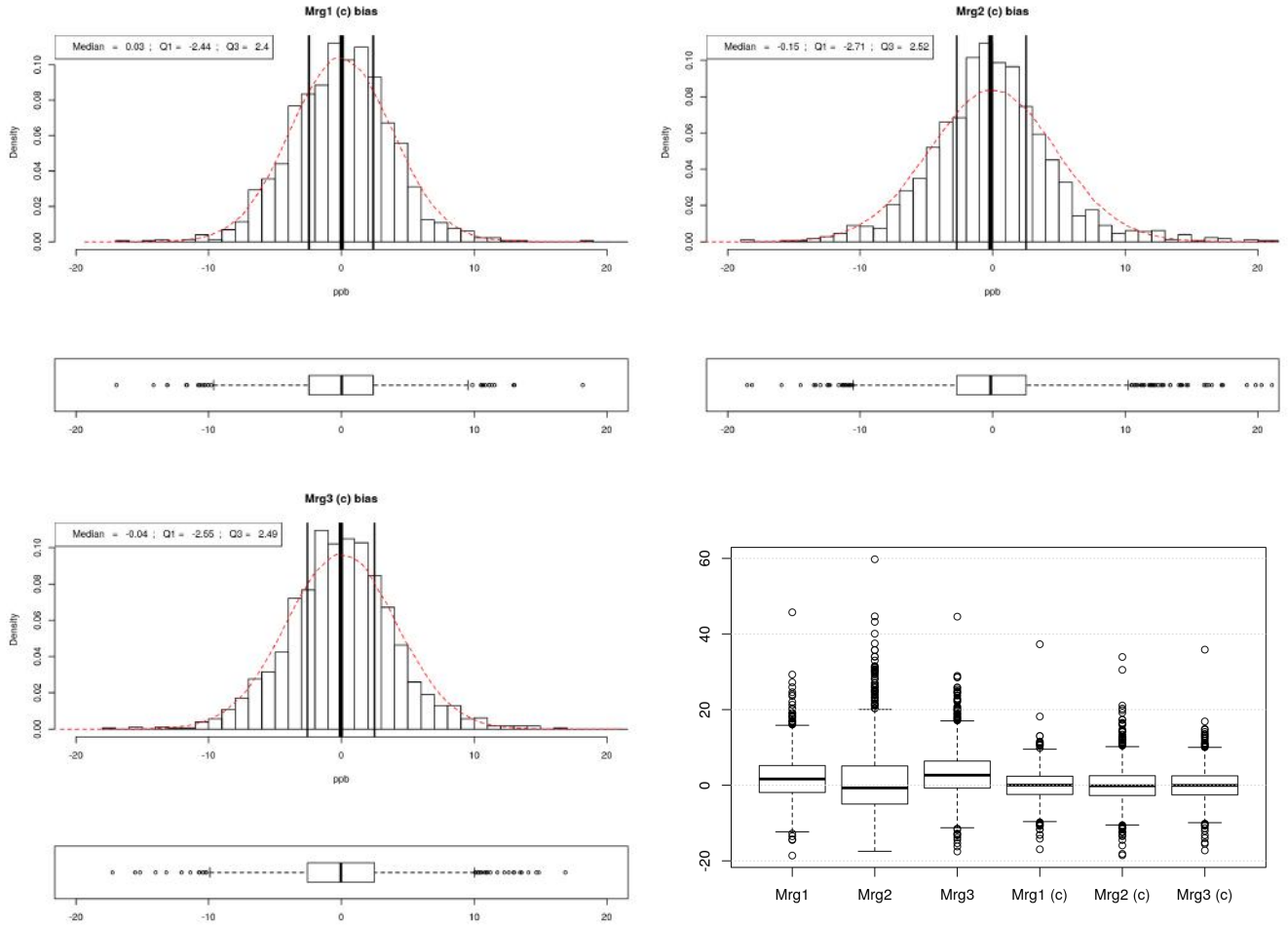
Figure 5. In order from top-left to bottom-right: (A) bias between the reference instrument and the Mrg1 sensor after the LCS correction, (B) bias of the Mrg2 sensor after LCS correction, (C) bias of the Mrg3 sensor after correction and (D) comparison of the LCSs bias before and after correction.

3.6.3 Scenario 2a

We considered the average coefficient values and their relative standard deviations to model the bias of each sensor and to calculate the corrected LCS ozone dataset. In this scenario the inter-correlation between the LCSs and the reference improved by $\approx 1\%$. The accuracy between the LCSs measurements and the reference improved, lowering the average bias (MAE) to ≈ 3.3 ppb. The 50% of the bias distribution confidence interval (CI) was $\approx \pm 2.6$ ppb and the 95% CI was $\approx \pm 8.7$ ppb.
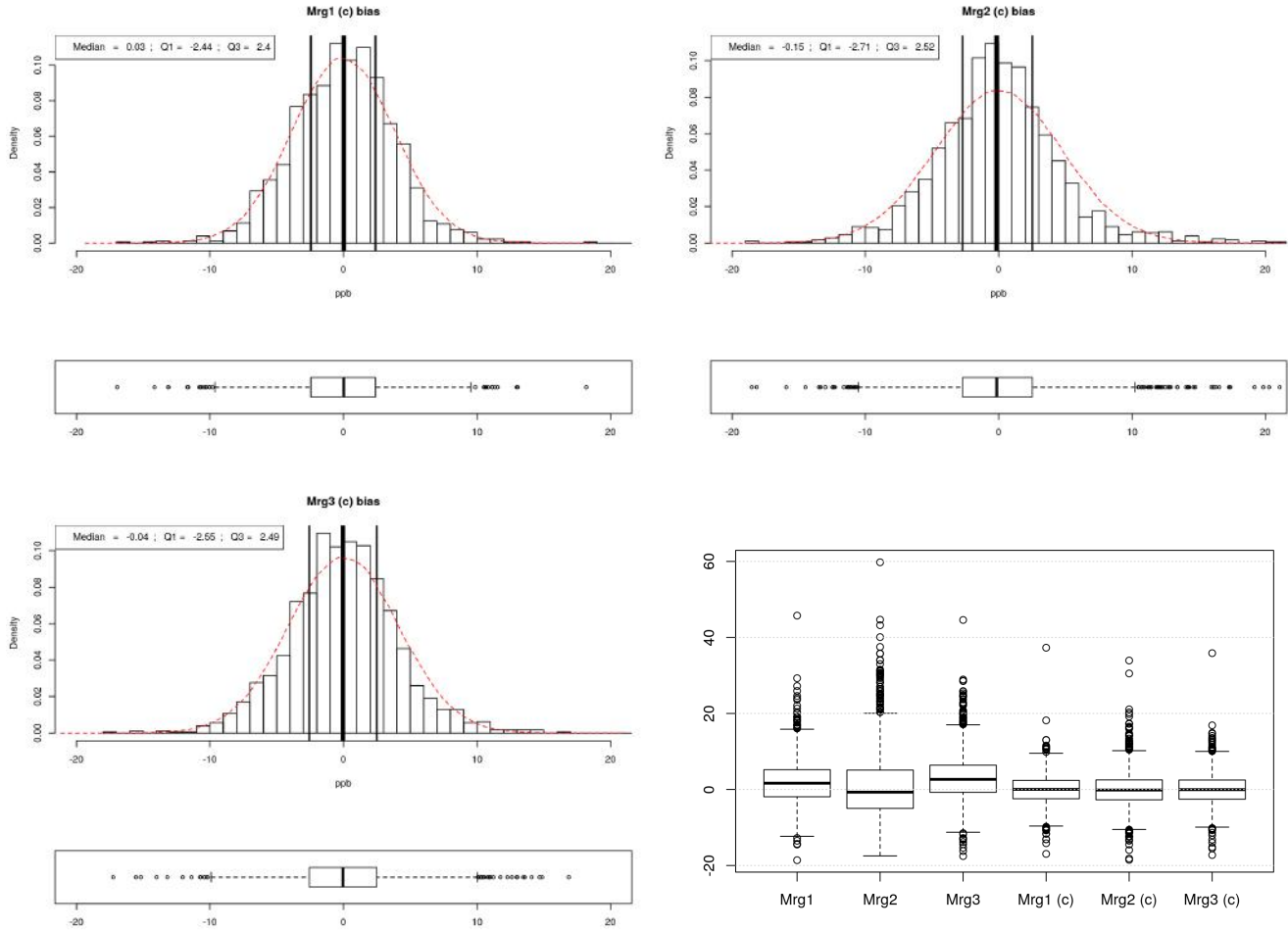
Figure 6. In order from top-left to bottom-right: (A) bias between the reference instrument and the Mrg1 sensor after the LCS correction, (B) bias of the Mrg2 sensor after LCS correction, (C) bias of the Mrg3 sensor after correction and (D) comparison of the LCSs bias before and after correction.

evaluated the accuracy between a LCS and the reference, correcting its LCS dataset using the averaged value of the other two LCSs coefficients (scenario 2b). The average value of the intercept coefficient (a_0) is -27.76 ± 8.94%. The average value of the temperature coefficient (a_1) is 0.26 ± 8.11%. The average value of the RH coefficient (a_2) is 0.11 ± 5.41% and the average values of the LCS coefficient (a_3) is 0.45 ± 11.32%.

3.6.3 Scenario 2a

We considered the average coefficient values and their relative standard deviations to model the bias of each sensor and to calculate the corrected LCS ozone dataset. In this scenario the inter-correlation between the LCSs and the reference improved

3.6.4 Scenario 2b

We corrected the ozone measurements of each low-cost sensor using the average model coefficients of the other two low-cost sensors. The inter-correlation metrics between the LCSs and the reference improved by $\approx 1\%$. The accuracy between the LCSs measurements and the reference improved, lowering the average bias (MAE) to ≈ 3.5 ppb. The 50% of the bias distribution CI was $\approx \pm 3$ ppb and the 95% CI was $\approx \pm 9$ ppb.

3.6.5 Scenario 3

The third scenario examined the execution of consequential field calibrations. It represents the situation where there is no chance to lay on local or remote calibration. The low-cost sensing system has to be installed alone, except for scheduled calibration periods during which a reference instrument is placed aside the low-cost sensor to model the bias. The calibrating periods must be chosen to depict as much as possible all the seasonal meteorological conditions of the site.

We modeled the bias considering only the June and the December reference dataset. These periods represent the annual extremes of the meteorological conditions at Col Margherita (Table 2). Data used for field calibration are 423 1-hr observations from the 30th of May to the 21st of Jun 2018 and 236 1-hr observations from the 1st to the 14th of December 2018.

In June the ambient temperature ranged from 2 °C to 14 °C with a mean temperature of 7 ± 2 °C, ambient relative humidity (RH) ranged from 48% to 100% with a mean RH of 85% $\pm$ 10%, atmospheric pressure ranged from 747 hPa to 755 hPa with a mean pressure of 750 ± 2 hPa and wind speed ranged from 0.20 m/s to 12 m/s with a mean wind speed of 3.5 ± 2 m/s. The range of 1-hour validated O_3 concentration was 31.3 ppb with a maximum of 66.3 ppb measured by the Thermo 49c Ozone analyzer.

In December the ambient temperature ranged from -16°C to 3 °C with a mean temperature of -6.5 ± 5 °C, RH ranged from 38% to 100% with a mean RH of 75% $\pm$ 15%, atmospheric pressure ranged from 734 hPa to 751 hPa with a mean pressure of 742 ± 5 hPa and wind speed ranged from 1 m/s to 23 m/s with a mean wind speed of 6 ± 4 m/s. The range of 1-hour validated O_3 concentration was 26.6 ppb with a maximum of 43.1 ppb measured by the Thermo 49c Ozone analyzer.

In this scenario the inter-correlation between the LCSs and the reference improved by $\approx 1\%$. The accuracy between the LCSs measurements and the reference improved by lowering the average bias (MAE) to ≈ 3.3 ppb. The 50% of the bias distribution CI was $\approx \pm 2.7$ ppb and the 95% CI was $\approx \pm 8.7$.

by $\approx 1\%$. The accuracy between the LCSs measurements and the reference improved, lowering the average bias (MAE) to ≈ 3.3 ppb. The 50% of the bias distribution confidence interval (CI) was $\approx \pm 2.6$ ppb and the 95% CI was $\approx \pm 8.7$ ppb.

3.6.4 Scenario 2b

We corrected the ozone measurements of each low-cost sensor using the average model coefficients of the other two low-cost sensors. The inter-correlation metrics between the LCSs and the reference improved by $\approx 1\%$. The accuracy between the LCSs measurements and the reference improved, lowering the average bias (MAE) to ≈ 3.5 ppb. The 50% of the bias distribution CI was $\approx \pm 3$ ppb and the 95% CI was $\approx \pm 9$ ppb.

3.6.5 Scenario 3

The third scenario examined the execution of consequential field calibrations. It represents the situation where there is no chance to lay on local or remote calibration. The low-cost sensing system has to be installed alone, except for scheduled calibration periods during which a reference instrument is placed aside the low-cost sensor to model the bias. The calibrating periods must be chosen to depict as much as possible all the seasonal meteorological conditions of the site.

We modeled the bias considering only the June and the December reference dataset. These periods represent the annual extremes of the meteorological conditions at Col Margherita (Table 2 and subsection S5.2). Data used for field calibration are 423 1-hr observations from the 30th of May to the 21st of Jun 2018 and 236 1-hr observations from the 1st to the 14th of December 2018.

In this scenario the inter-correlation between the LCSs and the reference improved by $\approx 1\%$. The accuracy between the LCSs measurements and the reference improved by lowering the average bias (MAE) to ≈ 3.3 ppb. The 50% of the bias distribution CI was $\approx \pm 2.7$ ppb and the 95% CI was $\approx \pm 8.7$.

		Scenario 1	Scenario 2a	Scenario 2b	Scenario 3
Mrg1	PCC	0.88	0.88	0.87	0.87
	MAE	2.95	3.02	3.32	2.97
	Median	0.03	0.01	0.94	0.14
	CI (95%)	-7.09 : 7.40	-7.89 : 7.12	-8.12 : 7.54	-7.36 : 7.66
Mrg2	PCC	0.80	0.80	0.80	0.79
	MAE	3.48	3.63	3.79	3.78
	Median	-0.15	-1.17	-1.24	-0.43
	CI (95%)	-9.32 : 10.92	-9.05 : 11.44	-8.65 : 13.01	-11.66 : 9.17
Mrg3	PCC	0.85	0.85	0.85	0.85
	MAE	3.13	3.29	3.24	3.25
	Median	-0.04	0.73	0.85	-0.75
	CI (95%)	-7.93 : 8.45	-8.06 : 8.46	-7.25 : 9.12	-9.15 : 7.25

Table 5. Summary of the performaces of the LCSs bias model in the three scenarios considered.

		Scenario 1	Scenario 2a	Scenario 2b	Scenario 3
Mrg1	PCC	0.88	0.88	0.87	0.87
	MAE	2.95	3.02	3.32	2.97
	Median	0.03	0.01	0.94	0.14
	CI (95%)	-7.09 : 7.40	-7.89 : 7.12	-8.12 : 7.54	-7.36 : 7.66
Mrg2	PCC	0.80	0.80	0.80	0.79
	MAE	3.48	3.63	3.79	3.78
	Median	-0.15	-1.17	-1.24	-0.43
	CI (95%)	-9.32 : 10.92	-9.05 : 11.44	-8.65 : 13.01	-11.66 : 9.17
Mrg3	PCC	0.85	0.85	0.85	0.85
	MAE	3.13	3.29	3.24	3.25
	Median	-0.04	0.73	0.85	-0.75
	CI (95%)	-7.93 : 8.45	-8.06 : 8.46	-7.25 : 9.12	-9.15 : 7.25

Table 5. Summary of the performaces of the LCSs bias model in the three scenarios considered. In Scenario 1 we corrected one LCS bias using its environmental model coefficients within the full dataset. In Scenario 2a we corrected a LCS bias averaging the environmental model coefficients of all the LCSs within the full dataset. In Scenario 2b we corrected a LCS bias averaging the environmental model coefficients of the others two LCSs within the full dataset. In Scenario 3 we corrected a LCS bias using the LCS calculated environmental model coefficients considering only the annual extremes meteorological conditions at Col Margherita. For each case are reported the final Pearson Correlation Coefficient (PCC) and Mean Absolute Error (MAE) between the low-cost sensor and the reference instrument, the bias distribution $Median$ and the bias distribution confidence interval (CI) at 95%.
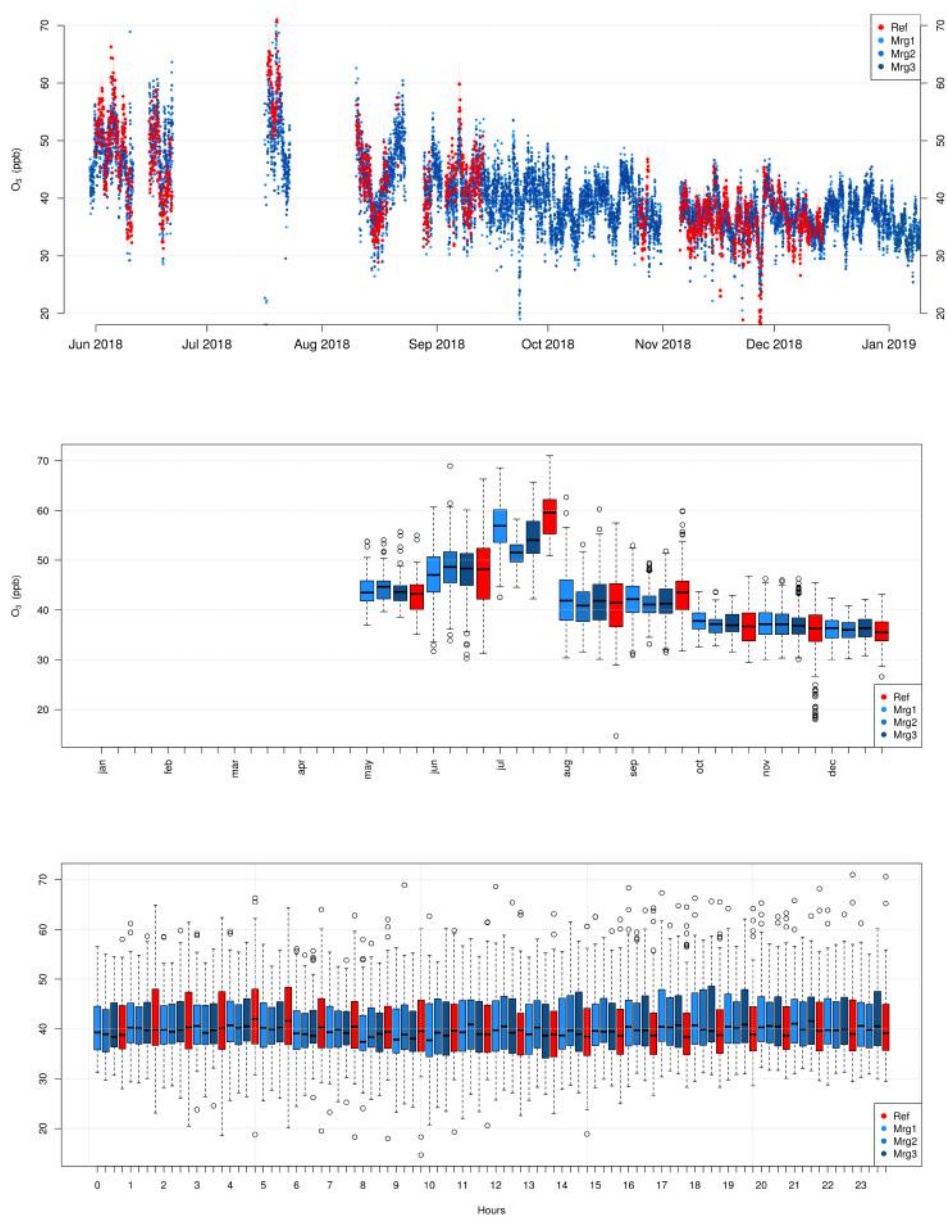
Figure 6. Time series of ozone concentration measurements and meteorological variables for the period June-December 2018. Monthly and hourly boxplots for the period June-December 2018. LCSs average values are reported in blue gradient and the reference ozone concentration is reported in red. Observations from periods where both the LCSs and the reference were operational have been considered for the monthly and hourly boxplots.

4 Discussion

We summarized the LCSs analytical performance results obtained through two laboratory calibration experiments and a ≈ 7 months field experiment performed at the Col Margherita observatory.

4.1 Detection limits

The LCSs were capable of detecting ozone in the typical environmental ppb range. During the laboratory calibration experiments we observed that the LOD of the LCSs was about 5 ppb and the LOQ was about 15 ppb. We noticed that the LCSs response to ozone concentration was linear ($PCC > 0.99$) up to 250 ppb and these analytical performances of the LCSs did not change after two laboratory calibration experiments, conducted three months apart one from another. When used in the field, the linear regression coefficients obtained through laboratory calibration, at fixed temperature and humidity, are not capable to fully describe the behavior of the LCSs ($PCC \approx 0.8$).

4.2 LCSs calibration

We observed that all the sensors require an individual double calibration (both in laboratory and in the field) and that the calibration values declared by the manufacturer could be insufficiently accurate for an environmental study. Attention should be used if deciding to perform a single field calibration (few days) since this can be insufficient: it is very unlikely that one single calibration excercise is representative of the environmental and meteorological condistions of a whole year. A solution, but increasing the logistic efforts and costs, might be to perform many field calibrations, covering at least the extremes of the meteorological year condition, in order to depict as much as possible the behavior of the sensors in the environment. An attractive solution might be to perform a remote calibration. We showed that we can improve the LCS accuracy using the bias correction coefficients optimized for other similar LCSs (Scenario 2b). Our results represent an "optimum-level" of performances since we used the entire dataset to derive the calibration coefficients and the performance of the remote calibrations was evaluated under very same meteorological and environmental condistions. Given this fascinating results, further studies on the accuracy and robustness of a remote calibration will be conducted.

4.3 Precision

The evaluation of the LCSs intra-correlation during the field experiment revealed that the sensors behave in a similar but not identical way ($intra-PCC \approx 0.9$), thus it is important to increase the reliability and reproducibility of the measurements considering LCSs redundancy. This is particularly important when using the sensors in the field without any reference. We detected indeed a case during which one of the three LCSs was not working properly (Supplementary Figure S2.3). These anomalies could not be detectable if redundancy is not considered. The precision of the LCSs, described by the RSD, was evaluated in the laboratory with a constant reference ozone concentration. We observed that near the LOD the LCSs RSD is ≈ 3.5%, decreasing to ≈ 1.6% at ≈ 50 ppb and reach the asymptotic value of ≈ 0.8% for larger ozone concentrations (> 200 ppb). We did not notice a deterioration of the LCSs precision between the two laboratory calibration experiments. During

4 Discussion

We summarized the LCSs analytical performance results obtained through two laboratory calibration experiments and a ≈ 7 months field experiment performed at the Col Margherita observatory.

4.1 Detection limits

The LCSs were capable of detecting ozone in the typical environmental ppb range. During the laboratory calibration experiments we observed that the LOD of the LCSs was about 5 ppb and the LOQ was about 15 ppb. We noticed that the LCSs response to ozone concentration was linear ($PCC > 0.99$) up to 250 ppb and these analytical performances of the LCSs did not change after two laboratory calibration experiments, conducted three months apart one from another. When used in the field, the linear regression coefficients obtained through laboratory calibration, at fixed temperature and humidity, are not capable to fully describe the behavior of the LCSs, $PCC \approx 0.8$.

4.2 LCSs calibration

We observed that all the sensors require an individual, both in laboratory and in the field, calibration and caution should be used if it is decided to rely on the declared calibration values, which could be insufficiently accurate for an environmental study, even if variation in ozone concentrations are clearly detectable. Careful should be used if deciding to perform a single field calibration since this can be insufficient as it is very unlikely that, at mid-latitudes, one could choose a representative period of the whole year. A solution might be to perform many field calibrations, covering at least the extremes of the meteorological year condition, in order to depict as much as possible the behavior of the sensors in the environment. It may be considered to perform a more exhaustive laboratory calibration in a climatic chamber simulating the environmental conditions where the sensor will be deployed, to improve the understanding of the LCSs.

4.3 Precision

The evaluation of the LCSs intra-correlation during the field experiment revealed that the sensors behave in a similar but not identical way ($intra - PCC \approx 0.9$), thus it is important to increase the reliability and reproducibility of the measurements considering LCSs redundancy. This is particularly important when using the sensors in the field without any reference. We detected indeed a case during which one of the three LCSs was not working properly (Supplementary Figure B3). These anomalies could not be detectable if redundancy is not considered. The precision of the LCSs, described by the RSD, was evaluated in the laboratory with a constant reference ozone concentration. We observed that near the LOD the LCSs RSD is $\approx 3.5\%$, decreasing to $\approx 1.6\%$ at ≈ 50 ppb and reach the asymptotic value of $\approx 0.8\%$ for larger ozone concentrations (> 200 ppb). We did not notice a deterioration of the LCSs precision between the two laboratory calibration experiments. During the field campaign it is not trivial to evaluate the precision in terms of RSD, because there is neither a constant reference ozone concentration nor a constant meteorological situation. Since we did not observe any deterioration of the LCSs precision

between the first and the second laboratory calibrations, we assumed that the sensor's precision has not been affected by the use in Col Margherita.

4.4 Bias

The LCSs average bias, measured through the MAE between the LCS and the reference instrument during the field experiment, was ≈ 3.5 ppb (≈ 6 ppb without performing the bias correction). The LCSs electrical noise measured in the laboratory was ≈ 1.5 ppb (see Supplementary Figure C1) and bias > 4 ppb. During the field experiment we observed that the LCSs bias is dependent from the air temperature, RH and from the LCS electrodes voltage. It is possible to build a multivariate linear model able to describe about 60% the bias variance during the period in which the LCSs operates aside the reference instrument. It is of interest that the environmental model coefficients do not differ much one from another ($\approx 8.5\%$). We noticed that it is possible to reduce the bias of one LCS using the average coefficient values of another LCS, suggesting the development of a remote field calibration of the sensors in the surrounding area of the observatory.

4.5 Reliability

We have not measured differences in the analytical performances between the two LCSs calibration experiments. We showed that during the field experiment the LCSs response to the reference ozone concentration was affected by the local meteorology and their dependence can be analytically described. We observed that a time dependent model for correcting the bias was not necessary for our field experiment, but would be reasonably needed for long-term monitoring, when LCSs aging will not be negligible. The rapid response (≈ 30 ppb $\cdot$ s^{-1}) and the small memory effect, measured both during the laboratory experiments and in the field experiment, allowed the measurement of rapid variations of the ozone concentration.

The sensor's datasheet reports that NO_2 interferes with the ozone measurements. Since at the MRG observatory there was not a NO_2 analyzer during our field experiment, we were not able to measure the concentration of this gaseous pollutant. We referred to a local study(Costantino, 2016) to guess the amount of NO_2. This work studied the data of the regional environmental Agency (ARPAV) report, which conducted a study on ozone and nitrogen dioxide from the 1st January 2007 to the 1st January 2011 at Passo Valles, located about 3.2 km away from the MRG, at 2.032 m a.s.l., about 500 m lower than MRG. From 2007 to 2011 the average annual concentration of NO_2 at Passo Valles was 4 ± 1 ppb. The average annual concentration of ozone at Passo valles was $\approx 94 \pm 5$ ppb, $\approx 45\%$ higher than the typical average concentration measured at MRG ($\approx 40 \pm 10$ ppb). It is worth to notice that the monitoring site in Passo Valles is closed to a road, which could be a local source of NO_2 pollution. Therefore, even if it was not possible to predict the NO_2 concentration at MRG, the mean values measured at Passo Valles suggest that a few ppb of NO_2 interference may have occurred during our field experiment in MRG. Considered all this, and since it has been observed that the NO_2 concentrations are decreasing all over Europe(Jamali et al., 2020; Castellanos and Boersma, 2012), it is unlikely that NO_2 interference could be easily detected by our LCSs system in MRG and used to explain part of the bias between the LCSs and the reference instrument.

We showed that the LCSs was subjected to many considerable "stresses" throughout the field experiment. During the summer period we faced some severe power outages which caused data losses. These events were due to heavy thunderstorms and bad

the field campaign it is not trivial to evaluate the precision in terms of RSD, because there is neither a constant reference ozone concentration nor a constant meteorological situation. Thus, since it is not possible to evaluate the precision in field, we assumed that the precision during the field experiments was compatible with the precision studied in the laboratory.

4.4 Bias

The LCSs average bias, measured through the MAE between the LCS and the reference instrument during the field experiment, was ≈ 3.5 ppb (≈ 6 ppb without performing the bias correction). The LCSs electrical noise measured in the laboratory was ≈ 1.5 ppb (see Supplementary Figure S3.1) and bias > 4 ppb. During the field experiment we observed that the LCSs bias is dependent from the air temperature, RH and from the LCS electrodes voltage. It is possible to build a multivariate linear model able to describe about 60% the bias variance during the period in which the LCSs operates in co-location with the reference instrument. It is of interest that the environmental model coefficients do not differ much one from another ($\approx 8.5\%$). We noticed that it is possible to reduce the bias of one LCS using the average coefficient values of another LCS, suggesting the possibility to perform a remote field calibration of the sensors in the surrounding area of the observatory.

4.5 Reliability

We have not measured differences in the analytical performances between the two LCSs calibration experiments. We showed that during the field experiment the LCSs response to the reference ozone concentration was affected by the local meteorology and their dependence can be analytically described. We observed that a time dependent model for correcting the bias was not necessary for our field experiment, but would be reasonably needed for long-term monitoring, when LCSs aging will not be negligible. The rapid response (≈ 30 ppb$\cdot$s^{-1}) and the small memory effect, measured both during the laboratory experiments and in the field experiment, allowed the measurement of rapid variations of the ozone concentration.

The sensor's datasheet reports that NO_2 interferes with the ozone measurements. Since at the MRG observatory there was not a NO_2 analyzer during our field experiment, we were not able to measure the concentration of this gaseous pollutant. We referred to a local study(Costantino, 2016) to deduce the amount of NO_2 that could have interfered with our experiment. This work was based on the data of the regional environmental agency: a survey on ozone and nitrogen dioxide at Passo Valles (2.032 m a.s.l., about 3.2 km away from the MRG and about 500 m of lower altitude than MRG) was conducted, from the 1st of January 2007 to the 1st of January 2011. The average annual concentration of NO_2 at Passo Valles was 2 ± 1 ppb and the average annual concentration of ozone was $\approx 47 \pm 3$ ppb. As a comparison, despite referring to different years, the ozone concentration at Col Margherita was $\approx 40 \pm 10$ ppb during 2018, $\approx 15\%$ lower than what was recorded at Passo Valles. It is worth to notice that the monitoring site at Passo Valles is next to a road, which could be a local source of NO_2 pollution. Therefore, even if it was not possible to know the NO_2 concentration at MRG, the mean values measured at Passo Valles suggest that a few ppb of NO_2 may have interfered with our experiment in MRG. Nevertheless, since it has been observed that among different years the NO_2 concentrations are decreasing all over Europe(Jamali et al., 2020; Castellanos and Boersma, 2012) with mean average values ranged from 0.15 to 0.36 ppb, while 25th and 50th percentiles ranged from 0.05 to 0.19 ppb,

370 weather conditions that are characteristic of the alpine summer season. Moreover, the LCSs faced a severe storm ("Vaia", 29th October 2018, see Supplementary Figure E1) which caused several damages all through the North of Italy and caused a general black out in the Col Margherita area. It is worth noticing that the LCSs system was the only one that remained on during the Vaia storm blackout. When the power returned, the system showed no damage.

365 and from 0.16 to 0.40 ppb respectively(Cristofanelli et al., 2021), it is unlikely that NO_2 interference could have been detected by our LCSs system in MRG and thus explain some of the bias we observed between the LCSs and the reference instrument.

We showed that the LCSs was subjected to many considerable "stresses" throughout the field experiment. During the summer period we faced some severe power outages which caused data losses. These events were due to heavy thunderstorms and bad weather conditions that are characteristic of the alpine summer season. Moreover, the LCSs faced a severe storm ("Vaia",

370 29th October 2018, see Supplementary Figure S5.1) which caused several damages all through the North of Italy and caused a general black out in the Col Margherita area. It is worth noticing that the LCSs system was the only one that remained on during the Vaia storm blackout. When the power returned, the system showed no damage.

5 Conclusions

We found that O_3 low-cost gas sensors can provide concentration measurements with a bias of few ppb (± 8.5 ppb at 95% of confidence) throughout the period of the field operation.

We remarked that all the sensors require an individual calibration. We observed that the laboratory calibration is not sufficient to explain the behavior of the sensors during the field experiment. As a consequence, performing a sensor field calibration near a reference site is necessary and this requires infrastructure. Since the quality of the sensor calibration depends on the description of the environmental conditions (i.e. pollutants concentrations, meteorology), the reference instrumentation is of primary importance. In this work we discussed three procedures for the LCSs field calibration which can be used for the design of a low-cost sensors network in an alpine region. We showed how to improve the LCSs analytical performances when the reference instrument is always present, when it is present only for scheduled calibration periods and finally how to improve the O_3 measurements of a standalone LCSs using a remote calibration.

The comparison with a reference grade instrument revealed that the sensor's bias is impacted by changes in environmental temperature and relative humidity. These effects are demonstrated to be reduced by the application of a correction function and we revealed that a multivariate linear model is capable of describing up to 70% of the bias variability. We noticed that the bias model coefficients were comparable between each sensor ($\approx 8.5\,\%$ of difference). This opens the chance to perform a remote calibration of low-cost sensors which are not in the proximity of the reference instrument. Future studies could focus on the improvement of the mathematical description of the LCSs working principle and on its environmental dependence, in order to evaluate to which extent a single bias model could be used in a sensors network in an alpine area.

Achievable technical improvements for the enhancement of the analytical performances of the LCSs system are still open as the low-cost technology is getting better. Considering an improved thermal insulation of the sensing system, while ensuring the circulation of the ambient air without impacting the energy efficiency of the instrument, might be taken into consideration for future works. This study reveals how to obtain valuable data from a low-cost instrument in a remote harsh alpine environment and shows procedures for the design of adequate monitoring strategies in the study of tropospheric gases in remote areas.

5   Conclusions

We found that O_3 low-cost gas sensors can provide concentration measurements with a bias of only a few ppb (± 8.5 ppb at

375   95% of confidence) throughout the period of field operation. We found that all the sensors required an individual calibration. We observed that laboratory calibration is not sufficient to explain the behavior of the sensors during this field experiment. Therefore, performing a sensor field calibration near a reference site is necessary and this requires infrastructure. Since the quality of the sensor calibration depends on the description of the environmental conditions (i.e. pollutant concentrations, meteorology), we showed that reference instrumentation is necessary for performing periodic field calibrations. In this work we

380   discussed three procedures for field calibration of the LCSs. We showed how to improve the LCSs analytical performance when a reference instrument is always present or when it is available for scheduled calibration periods. Finally, we showed how to improve O_3 measurements of standalone LCSs with remote calibration prototype. Comparison with a reference grade instrument revealed that the sensor's bias is impacted by changes in environmental temperature and relative humidity. These effects are can be reduced by applying a correction function and we showed that a multivariate linear model can describe up

385   to 60% of the bias variability. We noticed that the bias model coefficients were comparable between each sensor ($\approx 8.5\%$ of difference). Demonstrating the possibility of performing remote calibrations of low-cost sensors without a reference instrument. Future studies should focus on improvement of the mathematical description of the LCS working principle and on their environmental dependence, to evaluate to what extent a single bias model could be used for a sensors network in an alpine area. Achievable technical improvements for the enhancement of the analytical performance of the LCSs system are still

390   open as low-cost technology improves. Other improvements include an improved housing for the sensing system with thermal insulation and humidity control, whilst ensuring circulation of ambient air that does not impact the energy efficiency of the instrument. This study demonstrates how to obtain valuable ozone data from a low-cost instrument in a remote harsh high altitude alpine environment and shows procedures for the design of adequate monitoring strategies in the study of tropospheric gases in remote areas.

Data availability. The data used in this study can be obtained from the authors upon request.

Author contributions. Federico Dallo: Conceptualization, Data curation, Formal analysis, Methodology, Software, Writing - original draft, Writing - review & editing. Daniele Zannoni: Data curation, Formal analysis, Writing - review & editing. Jacopo Gabrieli: Conceptualization, Methodology, Writing - review & editing. Paolo Cristofanelli: Conceptualization, Writing - review & editing. Francescopiero Calzolari: Data curation. Fabrizio de Blasi: Data curation, Formal analysis, Writing - review & editing. Andrea Spolaor: Data curation, Writing - review & editing. Dario Battistel: Data curation, Writing - review & editing. Rachele Lodi: Data curation, Writing - review & editing. Warren R.L. Cairns: Writing - review & editing. Ann Mari Fjæraa: Conceptualization, Funding acquisition, Writing - review & editing. Paolo Bonasoni: Funding acquisition, Writing - review & editing. Carlo Barbante: Funding acquisition, Writing - review & editing.

Competing interests. The authors declare that they have no other competing interests.

Acknowledgements. We thank the European Commission for funding GMOS, as part of the FP7 (Contract no. 26511), during which the MRG observatory was built. The measurements of this study were supported by ERA-PLANET (www.era-planet.eu) and the trans-national project iGOSP - Integrated Global Observing Systems for Persistent Pollutants (www.igosp.eu), funded under the EU Horizon 2020-SC5-15-2015 "Strengthening the European Research Area in the domain of Earth Observation", type of action: ERA-NET-Cofund Grant, (Grant Agreement N. 689443). We thank for the financial support given by the National Project of Interest Next-Data (http://www.nextdataproject.it/) by the Italian Ministry for Education, University and Research (MIUR), for the ozone and meteorological measurements. This work was part of the O3NET project, funded by the Research Council of Norway through an Arctic Field Grant (ES607473, Research in Svalbard ID: 10940) We kindly thank Enrico Natin and Roberto Epis, form the Workshop of the Ca' Foscari University, and Roberto Marin, from the Area Servizi Informatici e Telecomunicazioni of the Ca' Foscari University for their technical support. We thank Meteotrentino for providing the solar radiation and precipitation data from the weather station of the Passo Valles (Trento, Italy) (https://www.meteotrentino.it). Finally, a special thank to Renzo Minella, Loris Scola and the "Ski area San Pellegrino" people (https://www.ski area sanpellegrino.it) for their fundamental cooperation and support during the field activities at the Col Margherita Observatory.

Data availability. The data used in this study can be obtained from the authors upon request.

Author contributions. Federico Dallo: Conceptualization, Funding acquisition, Data curation, Formal analysis, Methodology, Software, Writing - original draft, Writing - review & editing. Daniele Zannoni: Data curation, Formal analysis, Writing - review & editing. Jacopo Gabrieli: Conceptualization, Methodology, Writing - review & editing. Paolo Cristofanelli: Conceptualization, Writing - review & editing. Francescopiero Calzolari: Data curation. Fabrizio de Blasi: Data curation, Formal analysis, Writing - review & editing. Andrea Spolaor: Data curation, Writing - review & editing. Dario Battistel: Data curation, Writing - review & editing. Rachele Lodi: Data curation, Writing - review & editing. Warren R.L. Cairns: Writing - review & editing. Ann Mari Fjæraa: Conceptualization, Funding acquisition, Writing - review & editing. Paolo Bonasoni: Funding acquisition, Writing - review & editing. Carlo Barbante: Funding acquisition, Writing - review & editing.

Competing interests. The authors declare that they have no other competing interests.

Acknowledgements. We thank the European Commission for funding GMOS, as part of the FP7 (Contract no. 26511), during which the MRG observatory was built. The measurements of this study were supported by ERA-PLANET (www.era-planet.eu) and the trans-national project iGOSP - Integrated Global Observing Systems for Persistent Pollutants (www.igosp.eu), funded under the EU Horizon 2020-SC5-15-2015 "Strengthening the European Research Area in the domain of Earth Observation", type of action: ERA-NET-Cofund Grant, (Grant Agreement N. 689443). We thank for the financial support given by the National Project of Interest Next-Data (http://www.nextdataproject.it/) by the Italian Ministry for Education, University and Research (MIUR), for the ozone and meteorological measurements. This work was part of the O3NET project, funded by the Research Council of Norway through an Arctic Field Grant (ES607473, Research in Svalbard ID: 10940). This project has received funding from the European Union's Horizon 2020 research and innovation programme under the Marie Skłodowska-Curie grant agreement No. 844526. We kindly thank Enrico Natin and Roberto Epis, form the Workshop of the Ca' Foscari University, and Roberto Marin, from the Area Servizi Informatici e Telecomunicazioni of the Ca' Foscari University for their technical support. We thank Meteotrentino for providing the solar radiation and precipitation data from the weather station of the Passo Valles (Trento, Italy) (https://www.meteotrentino.it). Finally, a special thank to Renzo Minella, Loris Scola and the "Ski area San Pellegrino" people (https://www.ski area sanpellegrino.it) for their fundamental cooperation and support during the field activities at the Col Margherita Observatory.

References

EuNetAir. Available online:, http://www.eunetair.it/, accessed: 2020-04-10.

Geoportal of the Alto-Adige province, a.

Geoportal of the Trentino province, b.

Andersen, M. P. and Culler, D. E.: System design trade-offs in a next-generation embedded wireless platform, in: Technical Report UCB/EECS-2014-162, EECS Department, University of California, Berkeley, 2014.

Andersen, M. P., Kim, H.-S., and Culler, D. E.: Hamilton: a cost-effective, low power networked sensor for indoor environment monitoring, in: Proceedings of the 4th ACM International Conference on Systems for Energy-Efficient Built Environments, pp. 1–2, 2017.

Barbante, C., Schwikowski, M., Döring, T., Gäggeler, H. W., Schotterer, U., Tobler, L., Van de Velde, K., Ferrari, C., Cozzi, G., Turetta, A., et al.: Historical record of European emissions of heavy metals to the atmosphere since the 1650s from Alpine snow/ice cores drilled near Monte Rosa, Environmental Science & Technology, 38, 4085–4090, 2004.

Barbaro, E., Morabito, E., Gregoris, E., Feltracco, M., Gabrieli, J., Vardè, M., Cairns, W. R., Dallo, F., De Blasi, F., Zangrando, R., et al.: Col Margherita Observatory: A background site in the Eastern Italian Alps for investigating the chemical composition of atmospheric aerosols, Atmospheric Environment, 221, 117 071, 2020.

Bauman, F., Webster, T., Zhang, H., Arens, E., Lehrer, D., Dickerhoff, D., Feng, J. D., Heinzerling, D., Fannon, D., Yu, T., et al.: Advanced Integrated Systems Technology Development, 2013.

Bonasoni, P., Laj, P., Angelini, F., Arduini, J., Bonafe, U., Calzolari, F., Cristofanelli, P., Decesari, S., Facchini, M., Fuzzi, S., et al.: The ABC-Pyramid Atmospheric Research Observatory in Himalaya for aerosol, ozone and halocarbon measurements, Science of the Total Environment, 391, 252–261, 2008.

Borrego, C., Costa, A., Ginja, J., Amorim, M., Coutinho, M., Karatzas, K., Sioumis, T., Katsifarakis, N., Konstantinidis, K., De Vito, S., et al.: Assessment of air quality microsensors versus reference methods: The EuNetAir joint exercise, Atmospheric Environment, 147, 246–263, 2016.

Borrego, C., Ginja, J., Coutinho, M., Ribeiro, C., Karatzas, K., Sioumis, T., Katsifarakis, N., Konstantinidis, K., De Vito, S., Esposito, E., et al.: Assessment of air quality microsensors versus reference methods: The EuNetAir Joint Exercise–Part II, Atmospheric environment, 193, 127–142, 2018.

Brockwell, P. J., Davis, R. A., and Fienberg, S. E.: Time series: theory and methods: theory and methods, Springer Science & Business Media, 1991.

Castell, N., Kobernus, M., Liu, H.-Y., Schneider, P., Lahoz, W., Berre, A. J., and Noll, J.: Mobile technologies and services for environmental monitoring: The Citi-Sense-MOB approach, Urban climate, 14, 370–382, 2015.

Castellanos, P. and Boersma, K. F.: Reductions in nitrogen oxides over Europe driven by environmental policy and economic recession, Scientific reports, 2, 265, 2012.

Cleveland, W., Grosse, E., and Shyu, W.: Local regression models. Chapter 8 in Statistical models in S (JM Chambers and TJ Hastie eds.), 608 p, Wadsworth & Brooks/Cole, Pacific Grove, CA, 1992.

Committee, A. M. et al.: Recommendations for the definition, estimation and use of the detection limit, Analyst, 112, 199–204, 1987.

Cooper, O. R., Parrish, D., Ziemke, J., Cupeiro, M., Galbally, I., Gilge, S., Horowitz, L., Jensen, N., Lamarque, J.-F., Naik, V., et al.: Global distribution and trends of tropospheric ozone: An observation-based review, 2014.

References

420 EuNetAir. Available online:, http://www.eunetair.it/, accessed: 2020-04-10.

Geoportal of the Alto-Adige province, a.

Geoportal of the Trentino province, b.

Andersen, M. P. and Culler, D. E.: System design trade-offs in a next-generation embedded wireless platform, in: Technical Report UCB/EECS-2014-162, EECS Department, University of California, Berkeley, 2014.

425 Andersen, M. P., Kim, H.-S., and Culler, D. E.: Hamilton: a cost-effective, low power networked sensor for indoor environment monitoring, in: Proceedings of the 4th ACM International Conference on Systems for Energy-Efficient Built Environments, pp. 1–2, 2017.

Barbante, C., Schwikowski, M., Döring, T., Gäggeler, H. W., Schotterer, U., Tobler, L., Van de Velde, K., Ferrari, C., Cozzi, G., Turetta, A., et al.: Historical record of European emissions of heavy metals to the atmosphere since the 1650s from Alpine snow/ice cores drilled near Monte Rosa, Environmental Science & Technology, 38, 4085–4090, 2004.

430 Barbaro, E., Morabito, E., Gregoris, E., Feltracco, M., Gabrieli, J., Vardè, M., Cairns, W. R., Dallo, F., De Blasi, F., Zangrando, R., et al.: Col Margherita Observatory: A background site in the Eastern Italian Alps for investigating the chemical composition of atmospheric aerosols, Atmospheric Environment, 221, 117 071, 2020.

Bauman, F., Webster, T., Zhang, H., Arens, E., Lehrer, D., Dickerhoff, D., Feng, J. D., Heinzerling, D., Fannon, D., Yu, T., et al.: Advanced Integrated Systems Technology Development, 2013.

435 Bonasoni, P., Laj, P., Angelini, F., Arduini, J., Bonafe, U., Calzolari, F., Cristofanelli, P., Decesari, S., Facchini, M., Fuzzi, S., et al.: The ABC-Pyramid Atmospheric Research Observatory in Himalaya for aerosol, ozone and halocarbon measurements, Science of the Total Environment, 391, 252–261, 2008.

Borrego, C., Costa, A., Ginja, J., Amorim, M., Coutinho, M., Karatzas, K., Sioumis, T., Katsifarakis, N., Konstantinidis, K., De Vito, S., et al.: Assessment of air quality microsensors versus reference methods: The EuNetAir joint exercise, Atmospheric Environment, 147, 246–263, 2016.

440

Borrego, C., Ginja, J., Coutinho, M., Ribeiro, C., Karatzas, K., Sioumis, T., Katsifarakis, N., Konstantinidis, K., De Vito, S., Esposito, E., et al.: Assessment of air quality microsensors versus reference methods: The EuNetAir Joint Exercise–Part II, Atmospheric environment, 193, 127–142, 2018.

Brockwell, P. J., Davis, R. A., and Fienberg, S. E.: Time series: theory and methods: theory and methods, Springer Science & Business Media, 1991.

445

Castell, N., Kobernus, M., Liu, H.-Y., Schneider, P., Lahoz, W., Berre, A. J., and Noll, J.: Mobile technologies and services for environmental monitoring: The Citi-Sense-MOB approach, Urban climate, 14, 370–382, 2015.

Castellanos, P. and Boersma, K. F.: Reductions in nitrogen oxides over Europe driven by environmental policy and economic recession, Scientific reports, 2, 265, 2012.

450 Cleveland, W., Grosse, E., and Shyu, W.: Local regression models. Chapter 8 in Statistical models in S (JM Chambers and TJ Hastie eds.), 608 p, Wadsworth & Brooks/Cole, Pacific Grove, CA, 1992.

Committee, A. M. et al.: Recommendations for the definition, estimation and use of the detection limit, Analyst, 112, 199–204, 1987.

Cooper, O. R., Parrish, D., Ziemke, J., Cupeiro, M., Galbally, I., Gilge, S., Horowitz, L., Jensen, N., Lamarque, J.-F., Naik, V., et al.: Global distribution and trends of tropospheric ozone: An observation-based review, 2014.

Costantino, F.: Qualità dell'aria in cinque zone del Veneto: analisi attraverso stazioni di monitoraggio di background e di traffico, bachelor thesis, 2016.

Cristofanelli, P. and Bonasoni, P.: Background ozone in the southern Europe and Mediterranean area: influence of the transport processes, Environmental Pollution, 157, 1399–1406, 2009.

Cristofanelli, P., Bonasoni, P., Tositti, L., Bonafe, U., Calzolari, F., Evangelisti, F., Sandrini, S., and Stohl, A.: A 6-year analysis of stratospheric intrusions and their influence on ozone at Mt. Cimone (2165 m above sea level), Journal of Geophysical Research: Atmospheres, 111, 2006.

Crutzen, P. J., Lawrence, M. G., and Pöschl, U.: On the background photochemistry of tropospheric ozone, Tellus B: Chemical and Physical Meteorology, 51, 123–146, 1999.

Dobber, M. R., Dirksen, R. J., Levelt, P. F., van den Oord, G. H., Voors, R. H., Kleipool, Q., Jaross, G., Kowalewski, M., Hilsenrath, E., Leppelmeier, G. W., et al.: Ozone monitoring instrument calibration, IEEE Transactions on Geoscience and remote Sensing, 44, 1209–1238, 2006.

ESA: Fiducial Reference Measurements: FRM, https://earth.esa.int/web/sppa/activities/frm, accessed: 2020-04-10, 2020.

for Standardization, I. O.: Accuracy (trueness and Precision) of Measurement Methods and Results-Part 2: Basic Method for the Determination of Repeatability and Reproducibility of a Standard Measurement Method, International Organization for Standardization, 1994.

Forster, P., Ramaswamy, V., Artaxo, P., Berntsen, T., Betts, R., Fahey, D. W., Haywood, J., Lean, J., Lowe, D. C., Myhre, G., et al.: Changes in atmospheric constituents and in radiative forcing. Chapter 2, in: Climate Change 2007. The Physical Science Basis, 2007.

Gabrieli, J. and Barbante, C.: The Alps in the age of the Anthropocene: the impact of human activities on the cryosphere recorded in the Colle Gnifetti glacier, Rendiconti Lincei, 25, 71–83, 2014.

Gauss, M., Myhre, G., Pitari, G., Prather, M., Isaksen, I., Berntsen, T., Brasseur, G. P., Dentener, F., Derwent, R., Hauglustaine, D., et al.: Radiative forcing in the 21st century due to ozone changes in the troposphere and the lower stratosphere, Journal of Geophysical Research: Atmospheres, 108, 2003.

Hagan, D. H., Isaacman-VanWertz, G., Franklin, J. P., Wallace, L. M., Kocar, B. D., Heald, C. L., and Kroll, J. H.: Calibration and assessment of electrochemical air quality sensors by co-location with regulatory-grade instruments, 2018.

Harris, D. C.: Quantitative chemical analysis, Macmillan, 2010.

Heimann, I., Bright, V., McLeod, M., Mead, M., Popoola, O., Stewart, G., and Jones, R.: Source attribution of air pollution by spatial scale separation using high spatial density networks of low cost air quality sensors, Atmospheric Environment, 113, 10–19, 2015.

Hertel, O., Ketzel, M., Poulsen, M. B., Olsen, Y., Jensen, C. K., Ellermann, T., Jensen, S. S., Im, U., Ottosen, T.-B., Büttrich, S., et al.: Asessing the air pollution distribution in busy street of Copenhagen in the further development of a street pollution model, in: COST Action TD1105-New Sensing Technologies for Air-Pollution Control and Environmental Sustainability-Fifth Scientific Meeting, 2015.

Horwitz, W. and Albert, R.: Quality IssuesThe Concept of Uncertainty as Applied to ChemicalMeasurements, Analyst, 122, 615–617, 1997.

ISAC-CNR: Climate hotspots: atmospheric observations and technological development website:, http://www.isac.cnr.it/en/research_groups/climate-hotspots-atmospheric-observations-and-technological-development, accessed: 2020-04-10.

ISTAT: Censimento della popolazione e delle abitazioni, https://www.istat.it/it/censimenti-permanenti/censimenti-precedenti/popolazione-e-abitazioni/popolazione-2011, accessed: 2020-04-10, 2011.

Jacobson, M. Z. and Jacobson, M. Z.: Atmospheric pollution: history, science, and regulation, Cambridge University Press, 2002.

Jamali, S., Klingmyr, D., and Tagesson, T.: Global-Scale Patterns and Trends in Tropospheric NO2 Concentrations, 2005–2018, Remote Sensing, 12, 3526, 2020.

Costantino, F.: Qualità dell'aria in cinque zone del Veneto: analisi attraverso stazioni di monitoraggio di background e di traffico, bachelor thesis, 2016.

Cristofanelli, P. and Bonasoni, P.: Background ozone in the southern Europe and Mediterranean area: influence of the transport processes, Environmental Pollution, 157, 1399–1406, 2009.

Cristofanelli, P., Bonasoni, P., Tositti, L., Bonafe, U., Calzolari, F., Evangelisti, F., Sandrini, S., and Stohl, A.: A 6-year analysis of stratospheric intrusions and their influence on ozone at Mt. Cimone (2165 m above sea level), Journal of Geophysical Research: Atmospheres, 111, 2006.

Cristofanelli, P., Gutiérrez, I., Adame, J., Bonasoni, P., Busetto, M., Calzolari, F., Putero, D., and Roccato, F.: Interannual and seasonal variability of NOx observed at the Mt. Cimone GAW/WMO global station (2165 m asl, Italy), Atmospheric Environment, 249, 118 245, 2021.

Crutzen, P. J., Lawrence, M. G., and Pöschl, U.: On the background photochemistry of tropospheric ozone, Tellus B: Chemical and Physical Meteorology, 51, 123–146, 1999.

Diémoz, H., Barnaba, F., Magri, T., Pession, G., Dionisi, D., Pittavino, S., Tombolato, I. K., Campanelli, M., Ceca, L. S. D., Hervo, M., et al.: Transport of Po Valley aerosol pollution to the northwestern Alps–Part 1: Phenomenology, Atmospheric Chemistry and Physics, 19, 3065–3095, 2019.

Dobber, M. R., Dirksen, R. J., Levelt, P. F., van den Oord, G. H., Voors, R. H., Kleipool, Q., Jaross, G., Kowalewski, M., Hilsenrath, E., Leppelmeier, G. W., et al.: Ozone monitoring instrument calibration, IEEE Transactions on Geoscience and remote Sensing, 44, 1209–1238, 2006.

ESA: Fiducial Reference Measurements: FRM, https://earth.esa.int/web/sppa/activities/frm, accessed: 2020-04-10, 2020.

for Standardization, I. O.: Accuracy (trueness and Precision) of Measurement Methods and Results-Part 2: Basic Method for the Determination of Repeatability and Reproducibility of a Standard Measurement Method, International Organization for Standardization, 1994.

Forster, P., Ramaswamy, V., Artaxo, P., Berntsen, T., Betts, R., Fahey, D. W., Haywood, J., Lean, J., Lowe, D. C., Myhre, G., et al.: Changes in atmospheric constituents and in radiative forcing. Chapter 2, in: Climate Change 2007. The Physical Science Basis, 2007.

Gabrieli, J. and Barbante, C.: The Alps in the age of the Anthropocene: the impact of human activities on the cryosphere recorded in the Colle Gnifetti glacier, Rendiconti Lincei, 25, 71–83, 2014.

Gauss, M., Myhre, G., Pitari, G., Prather, M., Isaksen, I., Berntsen, T., Brasseur, G. P., Dentener, F., Derwent, R., Hauglustaine, D., et al.: Radiative forcing in the 21st century due to ozone changes in the troposphere and the lower stratosphere, Journal of Geophysical Research: Atmospheres, 108, 2003.

Hagan, D. H., Isaacman-VanWertz, G., Franklin, J. P., Wallace, L. M., Kocar, B. D., Heald, C. L., and Kroll, J. H.: Calibration and assessment of electrochemical air quality sensors by co-location with regulatory-grade instruments, 2018.

Harris, D. C.: Quantitative chemical analysis, Macmillan, 2010.

Heimann, I., Bright, V., McLeod, M., Mead, M., Popoola, O., Stewart, G., and Jones, R.: Source attribution of air pollution by spatial scale separation using high spatial density networks of low cost air quality sensors, Atmospheric Environment, 113, 10–19, 2015.

Hertel, O., Ketzel, M., Poulsen, M. B., Olsen, Y., Jensen, C. K., Ellermann, T., Jensen, S. S., Im, U., Ottosen, T.-B., Büttrich, S., et al.: Asessing the air pollution distribution in busy street of Copenhagen in the further development of a street pollution model, in: COST Action TD1105-New Sensing Technologies for Air-Pollution Control and Environmental Sustainability-Fifth Scientific Meeting, 2015.

Horwitz, W. and Albert, R.: Quality IssuesThe Concept of Uncertainty as Applied to ChemicalMeasurements, Analyst, 122, 615–617, 1997.

Jiang, X., Polastre, J., and Culler, D.: Perpetual environmentally powered sensor networks, in: IPSN 2005. Fourth International Symposium on Information Processing in Sensor Networks, 2005., pp. 463–468, IEEE, 2005.

Levis, P., Madden, S., Polastre, J., Szewczyk, R., Whitehouse, K., Woo, A., Gay, D., Hill, J., Welsh, M., Brewer, E., et al.: TinyOS: An operating system for sensor networks, in: Ambient intelligence, pp. 115–148, Springer, 2005.

Lewis, A., Peltier, W. R., and von Schneidemesser, E.: Low-cost sensors for the measurement of atmospheric composition: overview of topic and future applications, 2018.

Mead, M., Popoola, O., Stewart, G., Landshoff, P., Calleja, M., Hayes, M., Baldovi, J., McLeod, M., Hodgson, T., Dicks, J., et al.: The use of electrochemical sensors for monitoring urban air quality in low-cost, high-density networks, Atmospheric Environment, 70, 186–203, 2013.

Mueller, M., Meyer, J., and Hueglin, C.: Design of an ozone and nitrogen dioxide sensor unit and its long-term operation within a sensor network in the city of Zurich, Atmospheric Measurement Techniques, 10, 3783, 2017.

Naitza, L., Cristofanelli, P., Marinoni, A., Calzolari, F., Roccato, F., Busetto, M., Sferlazzo, D., Aruffo, E., Di Carlo, P., Bencardino, M., et al.: Increasing the maturity of measurements of essential climate variables (ECVs) at Italian atmospheric WMO/GAW observatories by implementing automated data elaboration chains, Computers & Geosciences, 137, 104 432, 2020.

O'Neill, A., Barber, D., Bauer, P., Dahlin, H., Diament, M., Hauglustaine, D., Le Traon, P., Mattia, F., Mauser, W., Merchant, C., et al.: Earth observation science strategy for ESA: a new era for scientific advances and societal benefits, Earth Observation Science Strategy, 2015.

Organization, W. M.: WMO Global Atmosphere Watch (GAW) Implementation Plan: 2016-2023, 2017.

Schultz, M. G., Schröder, S., Lyapina, O., Cooper, O. R., Galbally, I., Petropavlovskikh, I., Von Schneidemesser, E., Tanimoto, H., Elshorbany, Y., Naja, M., et al.: Tropospheric Ozone Assessment Report: Database and metrics data of global surface ozone observations, Elementa: Science of the Anthropocene, 5, 2017.

Sprovieri, F., Pirrone, N., Bencardino, M., D'Amore, F., Carbone, F., Cinnirella, S., Mannarino, V., Landis, M., Ebinghaus, R., Weigelt, A., et al.: Atmospheric mercury concentrations observed at ground-based monitoring sites globally distributed in the framework of the GMOS network, Atmospheric chemistry and physics, 16, 11 915, 2016.

Thompson, M.: Variation of precision with concentration in an analytical system, Analyst, 113, 1579–1587, 1988.

Tørseth, K., Aas, W., Breivik, K., Fjæraa, A. M., Fiebig, M., Hjellbrekke, A.-G., Lund Myhre, C., Solberg, S., and Yttri, K. E.: Introduction to the European Monitoring and Evaluation Programme (EMEP) and observed atmospheric composition change during 1972–2009, Atmospheric Chemistry and Physics, 12, 5447–5481, 2012.

Trentino, M.: Meteo Trentino Website, http://storico.meteotrentino.it/web.htm.

Veneto, R.: Geoportal of the Veneto region, https://idt2.regione.veneto.it/en/, accessed: 2020-04-10, 2020.

Young, P., Archibald, A., Bowman, K., Lamarque, J.-F., Naik, V., Stevenson, D., Tilmes, S., Voulgarakis, A., Wild, O., Bergmann, D., et al.: Pre-industrial to end 21st century projections of tropospheric ozone from the Atmospheric Chemistry and Climate Model Intercomparison Project (ACCMIP), 2013.

Zhang, W. and Director, W.: WMO integrated global observing system (WIGOS), Meteorological Monthly, 36, 1–8, 2010.

ISAC-CNR: Climate hotspots: atmospheric observations and technological development website:, http://www.isac.cnr.it/en/research_groups/climate-hotspots-atmospheric-observations-and-technological-development, accessed: 2020-04-10.

ISTAT: Censimento della popolazione e delle abitazioni, https://www.istat.it/it/censimenti-permanenti/censimenti-precedenti/popolazione-e-abitazioni/popolazione-2011, accessed: 2020-04-10, 2011.

Jacobson, M. Z. and Jacobson, M. Z.: Atmospheric pollution: history, science, and regulation, Cambridge University Press, 2002.

Jamali, S., Klingmyr, D., and Tagesson, T.: Global-Scale Patterns and Trends in Tropospheric NO2 Concentrations, 2005–2018, Remote Sensing, 12, 3526, 2020.

Jiang, X., Polastre, J., and Culler, D.: Perpetual environmentally powered sensor networks, in: IPSN 2005. Fourth International Symposium on Information Processing in Sensor Networks, 2005., pp. 463–468, IEEE, 2005.

Kim, J., Shusterman, A. A., Lieschke, K. J., Newman, C., and Cohen, R. C.: The Berkeley atmospheric CO 2 observation network: Field calibration and evaluation of low-cost air quality sensors, Atmospheric Measurement Techniques, 11, 1937–1946, 2018.

Levis, P., Madden, S., Polastre, J., Szewczyk, R., Whitehouse, K., Woo, A., Gay, D., Hill, J., Welsh, M., Brewer, E., et al.: TinyOS: An operating system for sensor networks, in: Ambient intelligence, pp. 115–148, Springer, 2005.

Lewis, A., Peltier, W. R., and von Schneidemesser, E.: Low-cost sensors for the measurement of atmospheric composition: overview of topic and future applications, 2018.

Masiol, M., Benetello, F., Harrison, R. M., Formenton, G., De Gaspari, F., and Pavoni, B.: Spatial, seasonal trends and transboundary transport of PM2. 5 inorganic ions in the Veneto region (Northeastern Italy), Atmospheric Environment, 117, 19–31, 2015.

Mead, M., Popoola, O., Stewart, G., Landshoff, P., Calleja, M., Hayes, M., Baldovi, J., McLeod, M., Hodgson, T., Dicks, J., et al.: The use of electrochemical sensors for monitoring urban air quality in low-cost, high-density networks, Atmospheric Environment, 70, 186–203, 2013.

Mueller, M., Meyer, J., and Hueglin, C.: Design of an ozone and nitrogen dioxide sensor unit and its long-term operation within a sensor network in the city of Zurich, Atmospheric Measurement Techniques, 10, 3783, 2017.

Naitza, L., Cristofanelli, P., Marinoni, A., Calzolari, F., Roccato, F., Busetto, M., Sferlazzo, D., Aruffo, E., Di Carlo, P., Bencardino, M., et al.: Increasing the maturity of measurements of essential climate variables (ECVs) at Italian atmospheric WMO/GAW observatories by implementing automated data elaboration chains, Computers & Geosciences, 137, 104 432, 2020.

O'Neill, A., Barber, D., Bauer, P., Dahlin, H., Diament, M., Hauglustaine, D., Le Traon, P., Mattia, F., Mauser, W., Merchant, C., et al.: Earth observation science strategy for ESA: a new era for scientific advances and societal benefits, Earth Observation Science Strategy, 2015.

Organization, W. M.: WMO Global Atmosphere Watch (GAW) Implementation Plan: 2016-2023, 2017.

Schultz, M. G., Schröder, S., Lyapina, O., Cooper, O. R., Galbally, I., Petropavlovskikh, I., Von Schneidemesser, E., Tanimoto, H., Elshorbany, Y., Naja, M., et al.: Tropospheric Ozone Assessment Report: Database and metrics data of global surface ozone observations, Elementa: Science of the Anthropocene, 5, 2017.

Sprovieri, F., Pirrone, N., Bencardino, M., D'Amore, F., Carbone, F., Cinnirella, S., Mannarino, V., Landis, M., Ebinghaus, R., Weigelt, A., et al.: Atmospheric mercury concentrations observed at ground-based monitoring sites globally distributed in the framework of the GMOS network, Atmospheric chemistry and physics, 16, 11 915, 2016.

Thompson, M.: Variation of precision with concentration in an analytical system, Analyst, 113, 1579–1587, 1988.

Tørseth, K., Aas, W., Breivik, K., Fjæraa, A. M., Fiebig, M., Hjellbrekke, A.-G., Lund Myhre, C., Solberg, S., and Yttri, K. E.: Introduction to the European Monitoring and Evaluation Programme (EMEP) and observed atmospheric composition change during 1972–2009, Atmospheric Chemistry and Physics, 12, 5447–5481, 2012.

530 Trentino, M.: Meteo Trentino Website, http://storico.meteotrentino.it/web.htm.

Veneto, R.: Geoportal of the Veneto region, https://idt2.regione.veneto.it/en/, accessed: 2020-04-10, 2020.

Young, P., Archibald, A., Bowman, K., Lamarque, J.-F., Naik, V., Stevenson, D., Tilmes, S., Voulgarakis, A., Wild, O., Bergmann, D., et al.: Pre-industrial to end 21st century projections of tropospheric ozone from the Atmospheric Chemistry and Climate Model Intercomparison Project (ACCMIP), 2013.

535 Zhang, W. and Director, W.: WMO integrated global observing system (WIGOS), Meteorological Monthly, 36, 1–8, 2010.